iScience

Article

PGR-mediated transcriptome identifies SOX9 as a critical regulator of progesterone production in human ovulatory follicles

Graphical abstract

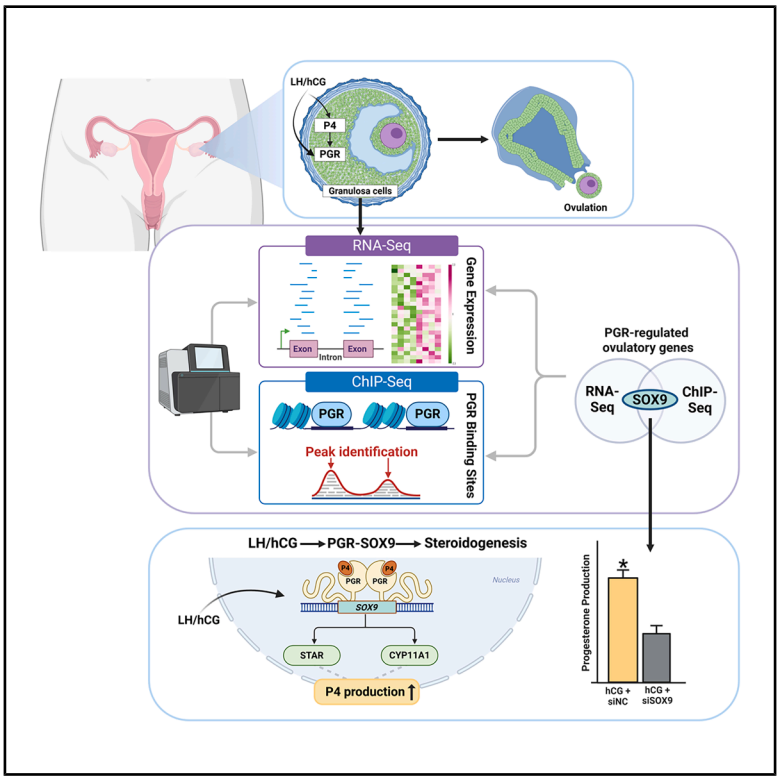

Highlights

- PGR-regulated transcriptome is defined in human ovulatory granulosa cells
- PGR regulates metabolism, steroidogenesis, and cell cycle pathways
- SOX9 is identified as ovulatory hCG-induced, PGR-regulated genes
- SOX9 controls progesterone production through regulation of steroidogenic genes

Authors

Hayce Jeon, Yohan Choi, Mats Brännström, James W. Akin, Thomas E. Curry, Jr., Misung Jo

Correspondence

mjo2@uky.edu

In brief

Biological sciences; Endocrinology; Reproductive medicine

Jeon et al., 2026, iScience *29*, 116044
June 19, 2026
https://doi.org/10.1016/j.isci.2026.116044

CellPress

iScience

CellPress
OPEN ACCESS

Article

PGR-mediated transcriptome identifies SOX9 as a critical regulator of progesterone production in human ovulatory follicles

Hayce Jeon,[1,2] Yohan Choi,[1] Mats Brännström,[3] James W. Akin,[4] Thomas E. Curry, Jr.,[1] and Misung Jo[1,5,*]
[1]Department of Obstetrics and Gynecology, University of Kentucky College of Medicine, Lexington, KY 40536, USA
[2]Department of Pharmacology and Nutritional Sciences, University of Kentucky College of Medicine, Lexington, KY 40536, USA
[3]Department of Obstetrics and Gynecology, Institute of Clinical Science, Sahlgrenska Academy, University of Gothenburg, Gothenburg 416 85, Sweden
[4]Bluegrass Fertility Center, Baptist Health Lexington, Lexington, KY 40503, USA
[5]Lead contact
*Correspondence: mjo2@uky.edu
https://doi.org/10.1016/j.isci.2026.116044

SUMMARY

Despite the widespread use of progesterone or progesterone receptor (PGR) blockers as contraceptives, the complete set of PGR-regulated genes and their roles in human ovulatory follicles remain unidentified. Here, we identified the PGR-regulated transcriptome, revealing numerous genes involved in metabolism, steroidogenesis, signaling activation, cell cycle regulation, and transcriptional control during ovulation using integrative omics and a primary human granulosa cell model that recapitulates the *in vivo* ovulatory phenomenon. These results led us to discover SRY-box transcription factor 9 (*SOX9*) as a human-specific, PGR-target gene during ovulation. Further functional studies showed that SOX9 regulates the expression of steroidogenesis-related genes, impacting progesterone production. In summary, we mapped the full spectrum of PGR-responsive genes in human ovulatory follicles and identified SOX9 as a human-specific mediator of the ovulatory process. These data provide critical insights into PGR-regulated ovulatory pathways, laying the foundation for developing targeted therapeutic strategies for infertility treatment and contraception.

INTRODUCTION

Ovulation is a fundamental process for fertility. Initiated by the surge of luteinizing hormone (LH), it depends on a complex interplay of hormonal signals and transcriptional regulation to coordinate the molecular and cellular events that culminate in follicle rupture.[1,2] The midcycle LH surge triggers a cascade of signaling pathways that drive intrafollicular changes, including the hormonal shift from estradiol to progesterone (P4), significantly increasing P4 levels in follicular fluid. This increase in P4 is crucial for regulating the gene expression necessary for the successful release of the oocyte and subsequent luteinization of granulosa cells.[3]

P4 exerts its effect primarily through the activation of the progesterone receptor (PGR), a ligand-activated transcription factor that regulates the expression of a set of specific genes controlling various aspects of female reproductive physiology.[4–6] Upon binding to P4, PGRs dimerize and translocate to the nucleus, interacting with progesterone response elements (PREs) in the promoter regions of target genes, thereby modulating their transcriptional activation.[7]

The expression profile of *PGR* in the ovary is highly conserved across species, with selective and transient increases observed in the granulosa cells of preovulatory follicles following the LH surge or stimulation with human chorionic gonadotropin (hCG) at various time points.[8–11] In rodents, *PGR* expression is significantly up-regulated between 3 and 6 h after the LH surge or hCG stimulation.[10,12–14] In cows, *PGR* expression peaked at 6 h following gonadotropin-releasing hormone administration, which declined by 12 h and then increased again at 24 h.[15] In non-human primates, the expression of *PGR* was also biphasic, showing the highest expression at 12 h after hCG administration, which declined at 24 h and then slightly increased at 36 h.[16] Notably, our lab has demonstrated that in humans, *PGR* expression peaks 12–18 h after hCG in the granulosa cells of ovulatory follicles obtained from regularly cycling women.[8]

Multiple studies have demonstrated the pivotal role of the PGR signaling pathway in mediating the ovulation process. For instance, inhibiting PGR activity with antagonists such as mifepristone (RU486) or ulipristal acetate has been shown to delay or block ovulation in mice, rats, and humans.[17–20] In *Pgr*-null mice, ovulation is impaired due to defects in the degradation of the follicular wall, resulting in the entrapment of oocytes within luteinized follicles.[9] Additionally, knocking down the expression of *PGR* in macaque granulosa cells prevented follicle rupture and disrupted the rise in P4 levels.[21] Further investigation into the identification of downstream effectors of the PGR pathway has been conducted using animal models, primarily cultured bovine,

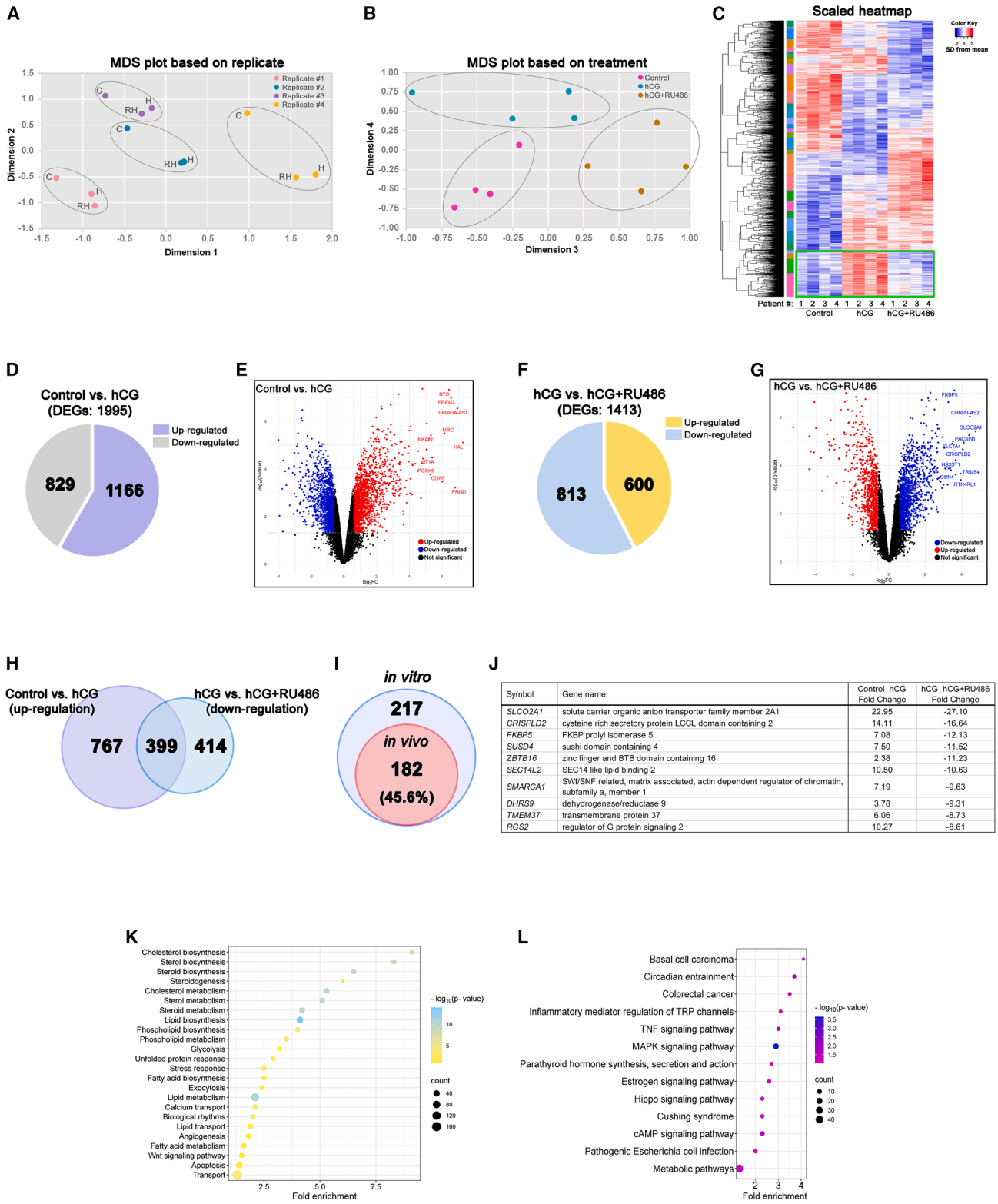

J

Symbol	Gene name	Control_hCG Fold Change	hCG_hCG+RU486 Fold Change
SLCO2A1	solute carrier organic anion transporter family member 2A1	22.95	-27.10
CRISPLD2	cysteine rich secretory protein LCCL domain containing 2	14.11	-16.64
FKBP5	FKBP prolyl isomerase 5	7.08	-12.13
SUSD4	sushi domain containing 4	7.50	-11.52
ZBTB16	zinc finger and BTB domain containing 16	2.38	-11.23
SEC14L2	SEC14 like lipid binding 2	10.50	-10.63
SMARCA1	SWI/SNF related, matrix associated, actin dependent regulator of chromatin, subfamily a, member 1	7.19	-9.63
DHRS9	dehydrogenase/reductase 9	3.78	-9.31
TMEM37	transmembrane protein 37	6.06	-8.73
RGS2	regulator of G protein signaling 2	10.27	-8.61

Figure 1. Identification of differentially regulated genes (DEGs) and PGR downstream targets in hGLCs

(A) MDS plot of gene expression profiles by replicate, with each color representing an individual patient sample across treatments: C (control), H (hCG), and RH (hCG + RU486).

(legend continued on next page)

equine, or rat granulosa cells treated with PGR antagonists.[15,22–24] With the advancement in the generation of different *Pgr* knockout (*Pgr*KO) mouse models and large-scale gene expression analyses, such as microarray and RNA sequencing (RNA-seq), research from multiple laboratories has generated a list of PGR-regulated genes by comparing differentially expressed genes (DEGs) between wild-type (WT) and *Pgr*KO mice.[9,25–27] More recently, Dinh et al. utilized chromatin immunoprecipitation sequencing (ChIP-seq) to map PGR-binding sites on DNA, revealing PGR direct target genes and its potential co-transcriptional regulators in mouse granulosa cells collected after hCG administration.[25,26]

Despite considerable research into the role of PGR in ovulation using animal models described earlier, species-specific differences in gene regulation limit the applicability of findings from animal studies to human biology. Moreover, there are significant gaps in our understanding of the role of PGR in human ovulatory follicles due to the lack of an experimental model that can mimic *in vivo* periovulatory changes in humans. To address this knowledge gap, we have established a primary human granulosa/lutein cell (hGLC) culture model that recapitulates the ovulatory hCG-induced increase in progesterone production and *PGR* expression *in vivo*.[8,28] Utilizing this culture model in combination with RU486, we investigated the LH/hCG-PGR-mediated pathway in human ovulatory follicles. By integrating RNA-seq and ChIP-seq datasets, we identified numerous ovulatory hCG-induced, PGR-regulated genes in human granulosa cells. Additionally, we performed a comparative analysis with the existing datasets from mouse studies to determine conserved and species-specific PGR-mediated ovulatory pathways between humans and mice. This comprehensive approach revealed SRY-box transcription factor 9 (*SOX9*) as a human-specific, ovulatory hCG-induced, and PGR-regulated gene in hGLCs. SOX9, a transcription factor critical for testis development, is highly expressed in the male gonad.[29] Conversely, *Sox9* expression is thought to be suppressed in the ovary to maintain the granulosa cell phenotype.[30,31] Therefore, we further characterized the expression profile of *SOX9* in granulosa cells isolated from dominant follicles or whole-follicle tissues obtained from regularly cycling women at different phases during the ovulatory period and investigated the regulatory mechanisms involved in *SOX9* expression and its potential roles using primary hGLCs.

RESULTS

Identification of PGR-regulated downstream genes in hGLCs

To identify the transcriptome regulated by PGR in hGLCs, we performed RNA-seq using hGLCs treated with vehicle (control), hCG alone, or hCG + RU486 for 12 h, which is the time point showing the peak expression of *PGR* both *in vivo* and *in vitro* in response to hCG.[8]

Multidimensional scaling (MDS) plots of our RNA-seq data revealed a distinct clustering of samples among each biological replicate (Figure 1A) and different treatments (Figure 1B). These findings indicate high consistency among each patient replicate and clear differentiation across the treatments, reflecting the significant impact of the experimental conditions in the gene expression. Consistent with the MDS plots, a heatmap of the RNA-seq data showed replicates in the same group with similar expression profiles, while distinct gene clusters emerged between treatments. For example, genes highlighted in the green-boxed region were up-regulated in samples treated with hCG alone but down-regulated in the hCG + RU486 group, providing a comprehensive view of the transcriptional changes induced by each treatment (Figure 1C).

Differential expression analysis of the RNA-seq data identified a total of 1,995 DEGs between the control and hCG-alone groups,

(B) MDS plot of gene expression profiles by treatment, with each color representing a different treatment. The number of dots in each color indicates the number of replicates used for each treatment.
(C) Heatmap of gene expression levels obtained from RNA-seq data. Each row represents a different gene, and each column corresponds to a sample, with four replicates per treatment. The numbers at the bottom represent each replicate sample. The color gradient indicates expression levels, with red representing higher expression and blue representing lower expression. The box highlights a cluster of genes that were up-regulated in hCG-treated samples but down-regulated in the hCG + RU486 group.
(D) Pie chart shows the differentially expressed genes (DEGs) in pairwise comparisons between hGLCs treated without (control) and with hCG for 12 h in RNA-seq analysis using the following criteria: q value < 0.05, |fold change (FC)| > 1.5, and Avg Expr> 0.
(E) Volcano plot of RNA-seq data showing the DEGs between control and hCG-treated hGLCs. Up-regulated genes (red), down-regulated genes (blue), and non-significant genes (black). A total of 15,367 genes are plotted, with the 10 most up-regulated genes labeled.
(F) Venn diagram of DEGs in hGLCs treated with hCG and hCG + RU486 at 12 h, identified using q value < 0.05, |fold change (FC)| > 1.5, and Avg Expr >0.
(G) Volcano plot of DEGs in hGLCs treated with hCG and hCG + RU486 for 12 h. Down-regulated genes (blue), up-regulated genes (red), and non-significant genes (black). A total of 16,596 genes are plotted, with the 10 most down-regulated genes labeled.
(H) Venn diagram illustrating hCG-upregulated and RU486-downregulated genes in hGLCs. The left circle (purple) represents genes up-regulated by hCG compared to control, while the right circle (blue) represents genes down-regulated by hCG + RU486 compared to hCG. The overlap indicates genes significantly up-regulated by hCG but down-regulated by RU486.
(I) Venn diagram showing that among 399 PGR-regulated genes, 182 genes are also found to be up-regulated after ovulatory induction in granulosa cells *in vivo* (Poulsen et al.[32]).
(J) List of the 10 most significantly down-regulated genes by RU486 from (I)(182 genes), ordered by fold change (FC) between hCG and hCG + RU486, including FC between control and hCG.
(K) Dot plot showing the biological process terms significantly enriched by 1,166 genes up-regulated by hCG vs. control at 12 h, with each term depicted by the number of associated genes (size), −log10(p value) (color), and fold enrichment (x axis).
(L) Dot plot illustrating the enriched KEGG pathways of 399 PGR-regulated genes from RNA-seq, with each pathway depicted by the number of associated genes (size), −log10(p value) (color), and fold enrichment (x axis).
hGLCs were treated without hCG or with hCG or hCG + RU486 for 12 h, followed by RNA-seq analysis. Four individual patient samples (replicates) were used across all treatments.

Table 1. IPA upstream regulator analysis of 1,166 genes up-regulated by hCG at 12 h

Upstream regulator[a]	Molecule type[b]	Fold change (C_H)[c]	Activation *Z* score[d]	*p* value of overlap[e]	# of regulated genes[f]
PGR	ligand-dependent nuclear receptor	3.933	3.350	3.34E−14	540
FOS	transcription regulator	8.112	2.773	7.96E−13	476
AMFR	transmembrane receptor	1.505	3.606	2.91E−12	319
XBP1	transcription regulator	1.869	4.957	2.41E−10	380
NCOA2	transcription regulator	1.712	4.077	1.60E−07	595
CEBPB	transcription regulator	2.856	5.999	2.62E−07	447
IGF1R	transmembrane receptor	2.003	4.777	8.57E−04	491
SOX9	transcription regulator	6.965	2.269	3.58E−03	462
KLF15	transcription regulator	5.296	2.095	8.33E−03	360

Table presenting the list of enriched upstream regulators identified by IPA upstream regulator analysis that are significantly up-regulated by hCG (1 IU/mL) at 12 h in our RNA-seq database, with criteria including *p* value < 0.01, activation state: activated, and molecule type: transcription regulator or receptor.

[a]Official symbol of the regulator.

[b]The type of the upstream regulator.

[c]The fold change in the expression of the upstream regulator induced by hCG, as observed in our RNA-seq data.

[d]A statistical measurement predicting the activation state of the upstream regulator, with positive values indicating activation.

[e]The statistical significance of the overlap between the dataset genes and the genes regulated by the upstream regulator (*p* value < 0.01).

[f]The number of genes in the dataset predicted to be regulated by the upstream regulator.

with 1,166 genes up-regulated and 829 genes down-regulated in response to hCG (Figure 1D; Table S2). The distribution of DEGs was visualized using a volcano plot, where up-regulated genes were shown in red and down-regulated genes in blue, with the top 10 most up-regulated genes labeled (Figure 1E; Table S3). The most up-regulated genes encode functional proteins, including a ligand of the transforming growth factor β (GDF6), a neuropeptide (NTS), enzymes involved in histidine metabolism (HAL), fatty acid metabolism (PCKS9), and sodium ion transport regulation (NKAIN1) (Figure 1E). Next, when comparing the hCG to the hCG + RU486-treated group, a total of 1,413 DEGs were identified, with 600 genes up-regulated and 813 genes down-regulated by hCG + RU486 (Figure 1F). The volcano plot highlighted the top 10 down-regulated genes in blue, including those encoding immunophilin (FKBP5) and transporters for prostaglandin (SLCO2A1) and amino acid (SLC7A4) (Figure 1G). To identify the list of genes downstream of the ovulatory hCG-PGR pathway, we overlapped the list of DEGs up-regulated by hCG compared to control with that of DEGs down-regulated by hCG + RU486 compared to hCG. Of the 1,166 genes up-regulated by hCG, 399 were significantly down-regulated by hCG + RU486 (Figure 1H; Table S4), revealing the subset of genes regulated by PGR. To determine whether the 399 genes (hCG-upregulated genes and RU486-downregulated genes) are also up-regulated after an ovulatory induction in granulosa cells *in vivo*, we compared our findings with the microarray dataset reported by Poulsen et al.,[32] which used granulosa cells collected at various time points after ovulatory induction from patients undergoing *in vitro* fertilization (IVF). Among the 399 identified PGR-regulated genes, 182 (45.6%) of them were also induced after ovulatory induction in their microarray data (Figure 1I; Table S4), including the 10 genes, such as key ovulatory genes like *SLCO2A1*, *FKBP5*, and *RGS2* (Figure 1J).

To understand the biological processes associated with the identified hCG-upregulated genes in our RNA-seq analysis, we performed Gene Ontology (GO) enrichment analysis using DAVID (version 6.8). There was significant enrichment of biological processes related to key aspects of ovulation, including the biosynthesis and metabolism of cholesterol, sterols, steroids, lipids, phospholipids, and fatty acids, as well as angiogenesis, glycolysis, and lipid transport (Figure 1K). Consistent with these findings, Kyoto Encyclopedia of Genes and Genomes (KEGG) pathway analysis showed that PGR-regulated genes were involved in metabolic pathways and other signaling pathways critical for ovarian function, such as TNF signaling, mitogen-activated protein kinase (MAPK) signaling, estrogen signaling, Hippo signaling, and cAMP signaling (Figure 1J). Ingenuity Pathway Analysis (IPA) upstream regulation analysis of the list of hCG-upregulated genes identified PGR as the most significant upstream regulator (Table 1), further supporting its role in mediating hCG-induced gene expression changes in human granulosa cells. In addition to PGR, the analysis identified other transcription factors crucial for normal reproductive function, including FOS, CEBPB, and SOX9 (Table 1).

Comparison of PGR-regulated genes in hGLCs and *Pgr*KO mouse granulosa cells

A previous study identified a set of PGR-regulated genes in mice granulosa cells by comparing the transcriptome collected at 8 h after hCG administration from *Pgr*KO with that of WT mice.[26] To determine the similarities in gene expression between mice and humans, the PGR-regulated genes (399 genes) in hGLCs were compared to those of *Pgr*KO mouse granulosa cells (638 genes, Table S6). The comparison revealed that only 31 genes were common to both datasets (Figure 2A). These include genes encoding a tight junction protein (CLDN3), a transcriptional coactivator (CITED1), Kruppel-like factors (KLF15 and KLF9), metallothionein (MT3), a prostaglandin transporter (SLCO2A1), and

A

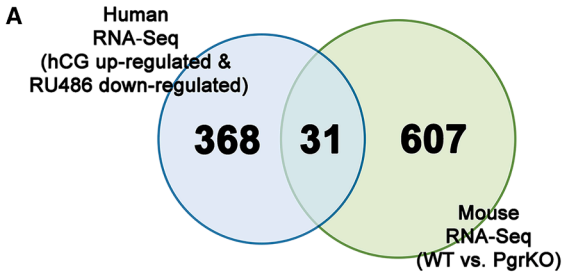

B

Human		Mouse	
Gene symbol	hCG_hCG+RU486 Fold Change	Gene symbol	WT_KO Fold Change
ABTB2	-6.44	*Abtb2*	-2.50
AMD1	-2.39	*Amd1*	-1.59
AMOTL1	-4.81	*Amotl1*	-1.65
APPL2	-6.18	*Appl2*	-2.72
CADPS2	-1.85	*Cadps2*	-2.19
CARMIL1	-3.74	*Carmil1*	-1.54
CITED1	-2.22	*Cited1*	-6.85
CLDN3	-6.33	*Cldn3*	-1.89
CRISPLD2	-16.64	*Crispld2*	-2.77
CYB5A	-1.98	*Cyb5a*	-1.76
DNM3	-4.53	*Dnm3*	-1.74
EFNB2	-3.67	*Efnb2*	-3.47
KLF15	-2.18	*Klf15*	-5.18
KLF9	-2.03	*Klf9*	-1.93
MERTK	-1.99	*Mertk*	-1.55
MOB3B	-2.54	*Mob3b*	-1.83
MT3	-1.85	*Mt3*	-2.36
PER1	-4.82	*Per1*	-1.56
PORCN	-4.31	*Porcn*	-4.38
RBBP7	-1.79	*Rbbp7*	-2.35
REEP1	-3.30	*Reep1*	-2.95
SFMBT2	-2.10	*Sfmbt2*	-1.64
SLC7A4	-17.34	*Slc7a4*	-2.25
SLCO2A1	-27.10	*Slco2a1*	-2.32
SMARCA1	-9.63	*Smarca1*	-1.87
SSBP2	-2.48	*Ssbp2*	-1.75
TMEM37	-8.73	*Tmem37*	-6.84
TNS1	-2.72	*Tns1*	-1.69
VCAN	-4.29	*Vcan*	-1.79
ZBTB16	-11.23	*Zbtb16*	-18.01

C

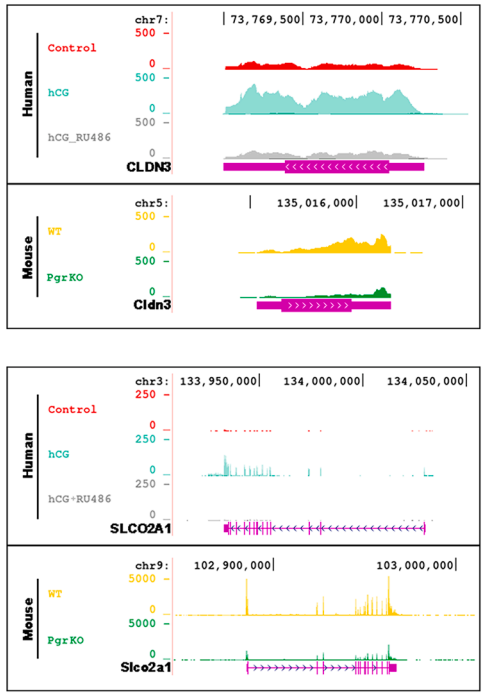

Figure 2. Comparison of PGR-regulated genes in hGLCs and *Pgr*KO mouse granulosa cells

(A) Venn diagram depicting the overlap of PGR-regulated genes in hGLCs (genes significantly up-regulated by hCG and down-regulated by RU486 at 12 h) and *Pgr*KO mouse granulosa cells (wild-type, WT vs. *Pgr*KO) at 8 h post-hCG. DEGs in the mouse dataset were selected based on a *q* value < 0.05 and |fold change (FC)| > 1.5, using the dataset published by Dinh et al.[26]

(B) List of 31 PGR-regulated genes common to both humans and mice, ordered alphabetically.

(C) The UCSC Genome Brower visualizes gene expression on *CLDN3* and *SLCO2A*. Tracks 1 to 3 display RNA-seq read coverage across the exons of *CLDN3* and *SLCO2A1*, showing expression levels under control, hCG, or hCG + RU486 in hGLCs. Tracks 4 and 5 show the expression level in granulosa cells of WT or *Pgr*KO mice. In all tracks, peak height represents expression levels.

an extracellular matrix proteoglycan (VCAN) (Figure 2B). To visualize these results, we examined *CLDN3*/*Cldn3* and *SLCO2A1*/*Slco2a1* transcripts from both datasets using the UCSC Genome Browser. Both genes displayed a marked up-regulation in the hCG-treated group compared to the control in hGLCs. In contrast, the expression levels of these genes were decreased in granulosa cells of both humans and mice when PGR activity was inhibited (hCG + RU486) and *Pgr* expression was ablated (*Pgr*KO), respectively (Figure 2C).

Identification of PGR-binding sites and PGR-regulated genes in hGLCs through integration of RNA-seq and PGR-ChIP-seq data

Our RNA-seq analysis identified a set of genes whose transcription is affected by RU486 in hGLCs by revealing transcriptional changes induced by the antagonism of PGR activity. However, differential expression analysis alone cannot determine direct regulatory relationships between PGR and its target genes. To uncover the underlying regulatory mechanisms driving these

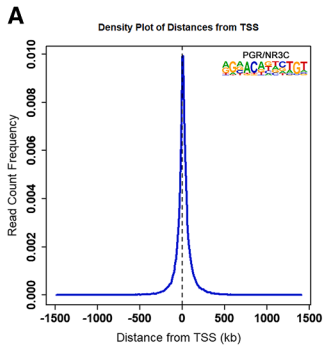

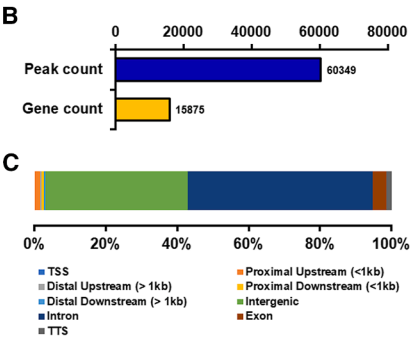

D

Genomic region	Percentage of total binding site (%)
Transcription start site (TSS)	0.003
Proximal Upstream (<1kb)	1.596
Distal Upstream (> 1kb)	0.418
Proximal Downstream (<1kb)	0.651
Distal Downstream (> 1kb)	0.403
Intergenic	39.759
Intron	51.920
Exon	3.747
Transcription termination site (TTS)	1.505

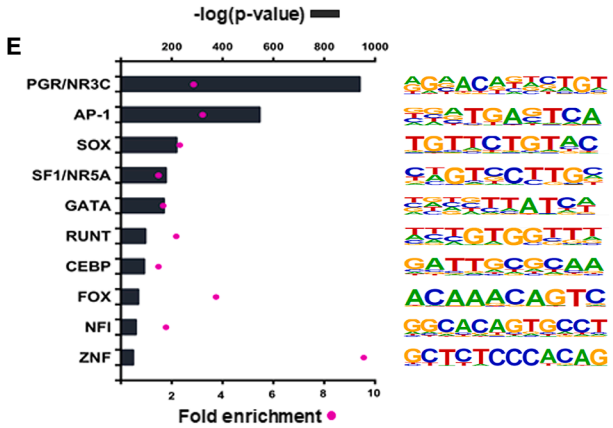

G

Gene symbol	Gene name	Control_hCG Fold Change	hCG_hCG+RU486 Fold Change	Function in the ovary
SLCO2A1	solute carrier organic anion transporter family member 2A1	22.95	-27.10	prostaglandin transporter, ovulation
FKBP5	FKBP prolyl isomerase 5	7.08	-12.13	steroid receptor regulation, ovarian steroidogenesis
ADAMTS9	ADAM metallopeptidase with thrombospondin type 1 motif 9	2.86	-6.04	extracellular matrix remodeling, follicle rupture, and ovulation
PTGES	prostaglandin E synthase	10.27	-5.22	prostaglandin biosynthesis, ovulation, angiogenesis
AREG	amphiregulin	10.21	-3.88	follicle development and ovulation
EREG	epiregulin	27.84	-3.88	follicle development and ovulation
BDNF	brain derived neurotrophic factor	4.35	-2.85	survival and growth of ovarian follicles, involved in oocyte maturation
HSD11B1	hydroxysteroid 11-beta dehydrogenase 1	7.64	-2.51	cortisol synthesis, ovulation, and luteinization
INHA	inhibin subunit alpha	3.12	-2.48	follicle development
HSD3B2	hydroxy-delta-5-steroid dehydrogenase, 3 beta- and steroid delta-isomerase 2	2.15	-1.94	ovarian steroidogenesis

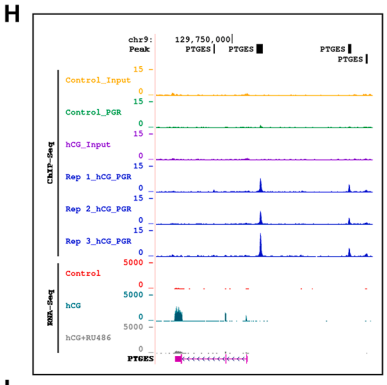

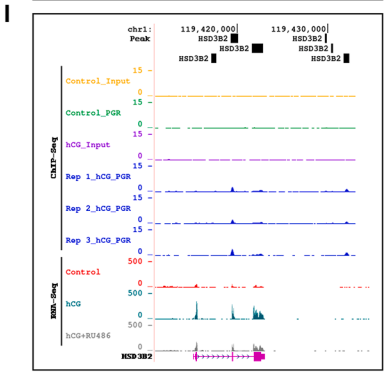

Figure 3. Identification of PGR-binding sites and PGR-regulated genes in hGLCs

(A) Density plot showing the distribution of PGR-ChIP-seq signal around transcription start sites (TSSs) in hGLCs at 12 h post-hCG. The *x* axis represents the distance from the TSS, with upstream regions to the left and downstream regions to the right. The *y* axis indicates the frequency of read counts for PGR peaks.

(B) Bar chart illustrating the total number of PGR-binding peaks and the corresponding genes in hGLCs treated with hCG for 12 h.

(C) Bar chart displaying the proportion of PGR peaks across different genomic regions.

(legend continued on next page)

transcriptional changes and to map PGR's genomic-binding sites, we performed ChIP-seq with an antibody against PGR in hGLCs treated with or without hCG for 12 h. We identified 60,349 enriched PGR-binding peaks across the genome that are associated with 15,875 distinct genes in hGLCs treated with hCG (Figure 3B; Table S7). PGR-binding sites were mostly distributed around 500 kb of transcription start sites (TSSs), as depicted in Figure 3A; however, only approximately 3% of peaks were located in the TSS region or its immediate vicinity, whether proximal or distal. The majority of the peaks were therefore found in other regions, such as intronic (51.92%) or intergenic areas (39.86%) (Figures 3C and 3D). The *de novo* motif analysis further revealed several highly enriched motifs within PGR-bound regions. As expected, the motif for PGR/NR3C was the most significantly enriched among identified motifs (Figure 3E). Additionally, motifs associated with the transcription factor family of AP-1, SOX, SF1/NR5A, GATA, RUNT, CEBP, FOX, NFI, and ZNF were also prominently enriched. This suggests these transcription factors' potential co-regulatory role in mediating the PGR-target gene transcription (Figure 3E).

To further elucidate whether PGR directly targets the genes identified as PGR regulated in RNA-seq, we integrated RNA-seq results with ChIP-seq data for a comprehensive analysis. Among the 399 PGR-regulated genes identified in the RNA-seq data, 302 genes were confirmed to have PGR-binding sites by ChIP-seq analysis (Figure 3F; Table S8). Notably, these targets included key ovulatory genes involved in prostaglandin synthesis and transport (*PTGES* and *SLCO2A1*), follicle maturation (*AREG*, *EREG*, *BDNF*, and *INHA*), follicle rupture (*ADAMTS9*), steroidogenesis (*HSD3B2* and *HSD11B1*), and steroid receptor regulation (*FKBP5*) (Figure 3G).

Genome browser tracks for *PTGES* and *HSD3B2* are provided to demonstrate these findings. RNA-seq data indicated that expression levels of *PTGES* and *HSD3B2* are higher in samples treated with hCG compared to control, and these levels were reduced by RU486 (Figures 3H and 3I). ChIP-seq data revealed enriched PGR-binding regions on *PTGES* and *HSD3B2* in the hCG-treated group compared to the control, with binding sites located near the promoter and exon, respectively (Figures 3H and 3I).

Comparative analysis of PGR-ChIP-seq data in granulosa cells between humans and mice

A previous study has characterized PGR binding on the genome in mouse granulosa cells through ChIP-seq analyses.[26] To examine evolutionary conservation and divergence, we compared our ChIP-seq data from humans to mouse data. Our analysis revealed that out of 60,349 PGR peaks identified in humans, 26,274 (43.5%) were conserved in the mouse dataset (Figure 4B). Both species exhibited a similar distribution of PGR-binding sites, with peaks located within 500 kb upstream or downstream of TSSs, as depicted by human peaks in blue and mouse peaks in yellow (Figure 4A). Moreover, there was approximately a 50% overlap in the gene counts associated with PGR peaks between two species (Figure 4B). Examples of overlapping genes include well-known ovulatory genes such as *ADAMTS9*, *CYP11A1*, *EGFR*, *FOS*, *HAS2*, *LYVE1*, *RUNX2*, *SNAP25*, *STAR*, and *VEGFA* (Figure 4C).

To further explore these conserved PGR-binding sites, we focused on *EGFR*/*Egfr* and *STAR*/*Star*, which showed overlapping PGR peaks in both species. Notably, the PGR-binding patterns on *EGFR*/*Egfr* varied between species. In humans, binding was enriched around the promoter region, while in mice, it extended from the intron to the transcription termination site (Figure 4D). For *STAR*/*Star*, PGR binding was observed near regulatory elements, specifically promoters, in both species (Figure 4D). These findings provide valuable insights into PGR-mediated gene regulation by revealing conserved binding sites shared between humans and mice and species-specific binding patterns.

SOX9 up-regulation after hCG administration in granulosa and cumulus cells of human periovulatory follicles

Based on our RNA-seq and ChIP-seq analyses, we identified *SOX9* as a direct downstream target of PGR in humans. Additionally, *SOX9* emerged as one of the significant upstream regulators of genes induced by hCG (Table 1), underscoring its potential role in mediating the PGR-regulated signaling pathway in human periovulatory follicles. SOX9 is primarily known for its role in sex determination and gene expression regulation across various tissues[29]; however, its specific role in human periovulatory follicles remains unexplored. To determine whether *SOX9* is expressed and regulated in human periovulatory follicles, we characterized its expression in dominant follicles retrieved before the LH surge or at defined hours after hCG administration, which was used to mimic the LH surge in regularly cycling women. The levels of mRNA for *SOX9* in granulosa cells were increased during the early ovulatory phase (10.6-fold) compared to the levels before the LH surge and then rapidly declined to pre-ovulatory levels during the late ovulatory phase (Figure 5A). Consistent with the mRNA profile, SOX9 staining was elevated in dominant follicles obtained during the early ovulatory phase after hCG stimulation (Figure 5C). Notably, SOX9 staining was

(D) Distribution of PGR-binding sites across the indicated genomic regions is expressed as a percentage of total binding sites.
(E) Top 10 *de novo* motifs enriched at PGR-binding sites. Bars represent −log10(*p* value), and circles indicate fold enrichment relative to the background.
(F) Venn diagram illustrating the overlap between the list of PGR-regulated genes identified by RNA-seq (Figure 1H) and PGR-bound genes identified by PGR ChIP-seq (B).
(G) List of 10 known ovulatory genes identified in both RNA-seq and PGR-ChIP-seq datasets, including fold changes in expression after hCG vs. control, fold changes in down-regulation upon PGR antagonism by RU486 vs. hCG, and their known functions in the ovary.
(H and I) PGR-binding sites and gene expression on *PTGES* and *HSD3B2* were visualized using the UCSC Genome Browser. Tracks 1 to 6 display PGR-binding peaks along the *PTGES* and *HSD3B2* gene loci in hGLCs treated without (control) or with hCG for 12 h. Peak height represents binding intensity, with the input track serving as a control for background noise for each treatment. Tracks 7 to 9 show RNA-seq read coverage across the *PTGES* and *HSD3B2* exons under control, hCG, or hCG + RU486 treatments, with peak height reflecting expression levels.

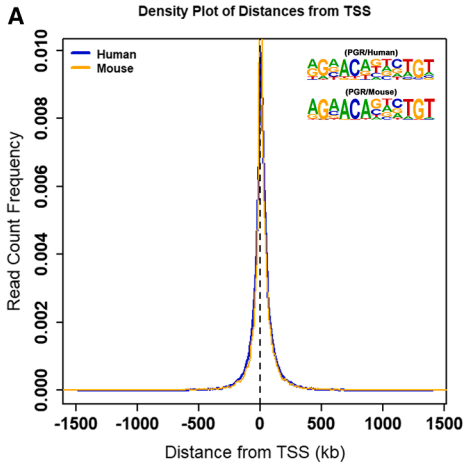

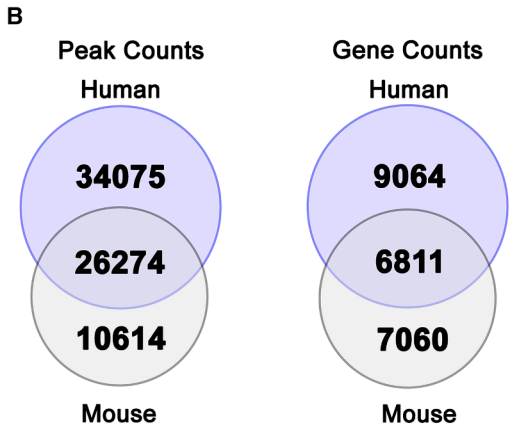

C

Gene symbol (Human)	Gene symbol (Mouse)	Gene name
ADAMTS1	*Adamts1*	ADAM metallopeptidase with thrombospondin type 1 motif 1
ADAMTS9	*Adamts9*	ADAM metallopeptidase with thrombospondin type 1 motif 9
AREG	*Areg*	Amphiregulin
CYP11A1	*Cyp11a1*	Cytochrome P450, family 11, subfamily A, member 1
CYP19A1	*Cyp19a1*	Cytochrome P450, family 19, subfamily A, member 1 (Aromatase)
CXCL12	*Cxcl12*	Chemokine (C-X-C motif) ligand 12 (SDF-1)
EDN2	*Edn2*	Endothelin 2
EGFR	*Egfr*	Epidermal growth factor receptor
EREG	*Ereg*	Epiregulin
FOS	*Fos*	FBJ osteosarcoma oncogene
HAS2	*Has2*	Hyaluronan synthase 2
IL6	*Il6*	Interleukin 6
LYVE1	*Lyve1*	Lymphatic vessel endothelial hyaluronan receptor 1
PGRMC1	*Pgrmc1*	Progesterone receptor membrane component 1
PTGES	*Ptges*	Prostaglandin E synthase
RUNX1	*Runx1*	Runt-related transcription factor 1
RUNX2	*Runx2*	Runt-related transcription factor 2
SNAP25	*Snap25*	Synaptosomal-associated protein 25
STAR	*Star*	Steroidogenic acute regulatory protein
VEGFA	*Vegfa*	Vascular endothelial growth factor A

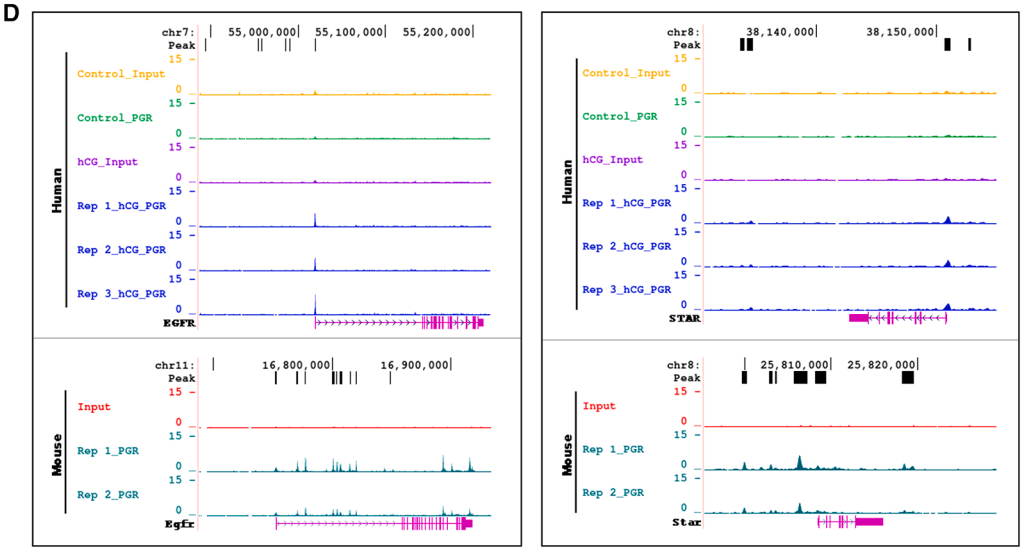

(legend on next page)

more prominent in granulosa cells than in the theca cell layer and appeared to be cytoplasmic in early ovulatory follicles (Figures 5C, b&f). Unlike mRNA levels, which were down-regulated during the late ovulatory phase, strong SOX9 staining persisted in granulosa cells of late ovulatory follicles, with predominant nuclear localization (Figures 5C, c&g). Even after ovulation, the strong staining for SOX9 remained in granulosa-lutein cells in post-ovulatory follicles (Figures 5C, d&h).

Next, to investigate whether *SOX9* is also expressed in cumulus cells of ovulatory follicles, cumulus granulosa cells and mural granulosa cells were collected from the patients undergoing IVF procedure at the time of oocyte retrieval (36 h after hCG administration). The levels of mRNA for *SOX9* were significantly higher in cumulus granulosa cells compared to those in mural granulosa cells from the same patient (Figure 5B).

Regulation of *SOX9* expression by PGR and the role of SOX9 in progesterone production and the expression of steroidogenic factors in hGLCs

To confirm that the *in vivo* induction of *SOX9* expression following hCG administration is directly mediated by hCG and PGR in human periovulatory follicles, we utilized the hGLC model. First, the cells were treated without (control) or with hCG at various time points to investigate the expression profile of *SOX9*. hCG treatment increased the levels of mRNA for *SOX9* compared to those in the control (Figure 6A). Consistent with the mRNA profile, protein levels of SOX9 were also increased in hCG-treated cells compared to control, with the highest levels observed at 24 h (Figure 6B). To assess the role of PGR, cells were treated with or without RU486 in the presence or absence of hCG for 12, 24, or 36 h to determine the effect of PGR antagonism on hCG-induced *SOX9* expression. As shown in Figures 6C and 6D, RU486 significantly attenuated hCG-induced increases in *SOX9* at both the mRNA and protein levels, reducing the expression to levels comparable to control. Notably, our RNA-seq data revealed that RU486 did not alter *LHCGR* mRNA at 12 h following hCG stimulation (Figure S1A), indicating that the suppression of *SOX9* mRNA by RU486 is not due to reduced *LHCGR* expression. Instead, this effect is mediated through the inhibition of PGR activity. Consistent with this interpretation, our RNA-seq and ChIP-seq data demonstrated reduced *PGR* mRNA expression following RU486 treatment and direct PGR binding on the *SOX9* locus (Figures 6E and S1B). Further experiments using a small interfering RNA (siRNA)-mediated knockdown approach also showed a trend toward reduced *SOX9* mRNA levels in *PGR* siRNA-treated hGLCs (p = 0.051), consistent with PGR-dependent control of *SOX9* transcription (Figure S2B).

Next, to investigate the role of *SOX9* in granulosa cells of human ovulatory follicles, we transfected the cells without (control) or with scrambled siRNA (negative control, siNC) or siRNA-targeting *SOX9* (siSOX9). Following transfection, the cells were treated with or without hCG (1 IU/mL) for an additional 24 or 36 h to assess the effects of *SOX9* knockdown on hCG-induced gene expression and progesterone production. As shown in Figure 6F, treatment with hCG + siNC significantly increased the level of *SOX9* mRNA compared to control. At 24 h after hCG treatment, siSOX9 treatment resulted in a significant reduction in levels of *SOX9* mRNA only at 50 nM but not at 10 nM compared to the levels observed with siNC. At 36 h, the levels of mRNA for *SOX9* were significantly decreased with both doses of siSOX9 compared to siNC (Figure 6F). Meanwhile, SOX9 protein was reduced in cells treated with 50 nM siSOX9 (Figures 6G and 6H), indicating the time- and dose-dependent knockdown of *SOX9* expression. Importantly, hCG-induced progesterone production was significantly reduced in the siSOX9 (50 nM)-treated cells (Figure 6I). Consistent with the hCG-induced progesterone production, hCG increased the expression of steroidogenic factors, such as *STAR*, *HSD3B*, and *CYP11A1* (Figures 6J and 6K). However, the increase in the expression of *STAR* and *CYP11A1*, but not HSD3B, was reduced in cells treated with *SOX9* siRNA (Figures 6J and 6K).

DISCUSSION

Successful ovulation depends on the precisely regulated transcription of various genes in preovulatory follicular cells, primarily mediated by transcription factors that are induced or activated by the LH surge or ovulatory hCG stimulation. Among these transcription factors, PGR has been established as essential for successful ovulation, as evident in the anovulatory phenotype of *Pgr*KO mice.[9,27] Our recent study demonstrated the induction of *PGR* expression in granulosa cells of human preovulatory follicles after ovulatory hCG administration.[8] In addition, *in vitro* studies using a PGR inhibitor, RU486, suggested that PGR is involved in various aspects of ovulation and luteinization in humans.[8,33,34] Utilizing an hGLC model that mimics the *in vivo* conditions of LH/hCG-induced P4 production and *PGR* expression and integrating RNA-seq and ChIP-seq approaches, the current study revealed a host of PGR-direct downstream target genes and potential co-transcriptional regulators with which PGR collaborates to control its downstream gene expressions. Of the PGR target genes, we identified *SOX9* as a human-specific ovulatory gene that plays an important role in steroidogenesis, likely acting as a transcriptional regulator in granulosa cells of periovulatory follicles.

Figure 4. Comparative analysis of PGR-ChIP-seq data in granulosa cells of humans and mice

(A) Density plot showing the distribution of PGR ChIP-seq signal around transcription start sites (TSSs) in granulosa cells of humans at 12 h post-hCG (blue line) and mice at 6 h post-hCG (yellow line). The *x* axis represents the distance from the TSS, with upstream regions to the left and downstream regions to the right. The *y* axis indicates the frequency of read counts for PGR peaks.

(B) Venn diagrams displaying the overlap of peak counts (left) and gene counts (right) between human and mouse PGR ChIP-seq datasets.

(C) List of 20 selected ovulatory genes among the overlapping genes.

(D) The PGR-binding sites on *EGFR*/*Egfr* and *STAR*/*Star* were visualized using the UCSC Genome Browser. Tracks 1 to 6 display PGR-binding peaks along the *EGFR* and *STAR* gene loci in hGLCs treated without (control) or with hCG for 12 h. Tracks 7 to 9 show PGR-binding peaks along the *Egfr* and *Star* gene loci in mouse granulosa cells treated with hCG for 6 h. Peak height represents binding intensity, and the input track serves as a control for background noise.

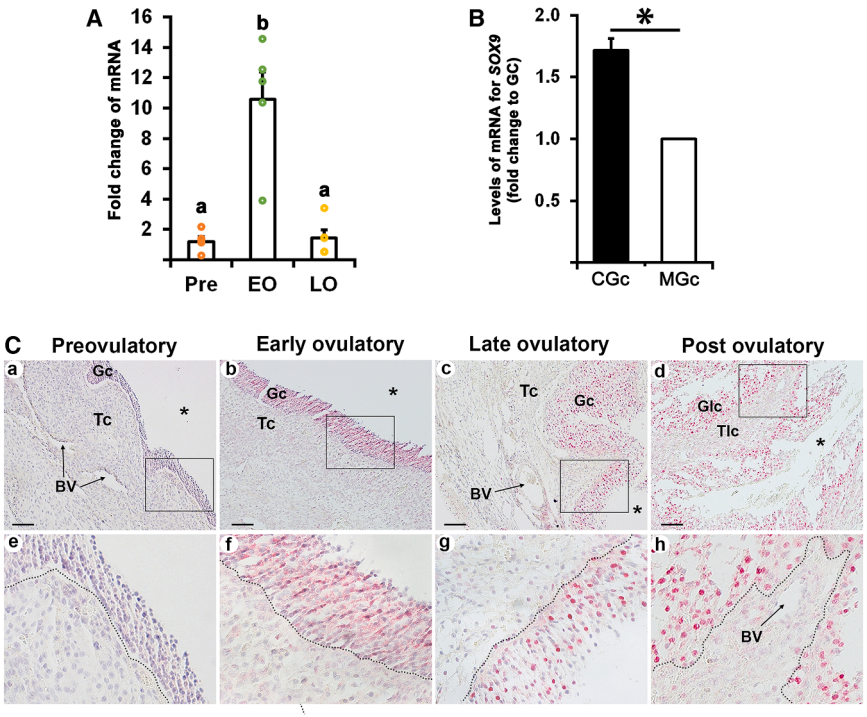

Figure 5. The expression of *SOX9* in granulosa and cumulus cells of human periovulatory follicles during the ovulatory period

(A) Dominant ovarian follicles were retrieved from women undergoing laparoscopic tubal sterilization before the LH surge or at defined hours after recombinant hCG administration and divided into four phases: pre (Pre), early (EO), late (LO), and post- (Post) ovulatory phase. *SOX9* mRNA levels in granulosa cells isolated from a dominant follicle collected at Pre, EO, and LO were measured using quantitative PCR (qPCR) and normalized to *GAPDH* mRNA levels in each sample. Results are presented as the mean ± SEM, with each dot representing an individual patient sample in each phase (n = 5/phase). Bars without common superscripts are significantly different ($p < 0.05$; one-way ANOVA, followed by Duncan's test).

(B) Cumulus granulosa cells (CGc) and mural granulosa cells (MGc) were collected at the time of oocyte retrieval from women undergoing an *in vitro* fertilization procedure. *SOX9* mRNA levels were measured using qPCR and normalized to *GAPDH* mRNA levels in each sample (n = 5 paired individual patient samples). *p = 0.002 (paired t test).

(C) Paraffin-embedded sections of dominant follicles (n = 2/Pre, n = 4/EO, n = 4/LO, n = 1/Post) were subjected to immunohistochemistry to detect SOX9. Pink staining indicates a positive signal, with SOX9 exhibiting predominantly in granulosa cells of early, late, and post-ovulatory follicles. Sections were lightly stained with hematoxylin (purple) for nuclear counterstaining. Gc, granulosa cells; Tc, theca cells; Glc, granulosa-lutein cells; Tlc, theca-lutein cells; BV, blood vessel. (*) indicates the antrum side of the follicle.

The boxed areas in (a), (b), (c), and (d) are shown at higher magnification in (e), (f), (g), and (h), respectively. Dotted lines in (e), (f), (g), and (h) indicate the boundary between the granulosa and theca cell compartments. Scale bars: 100 μm.

Since the discovery of PGR as an essential transcription factor for successful ovulation, research has focused on identifying its downstream targets using various animal models to uncover the LH surge/ovulatory hCG-induced PGR-mediated pathways that are necessary for ovulation.[9,14,25–27] Yet, in humans, unveiling these pathways has been challenging due to limited sample availability and ethical concerns. Therefore, our hGLC model provides a valuable alternative model for identifying hCG-induced transcriptomic changes and PGR-mediated pathways in human preovulatory follicles. Our RNA-seq data showed alterations in the expression profiles of numerous genes following hCG treatment and PGR-mediated regulatory shifts in these gene expressions. A previous study by Poulsen et al. has shown dynamic transcriptomic changes in human granulosa cells collected throughout the ovulatory period after ovulatory induction.[32] The comparison of our RNA-seq data on hGLCs and microarray data using *in vivo* granulosa cells revealed a nearly 50% overlap in the genes up-regulated by hCG and down-regulated by RU486 in human granulosa cells. This finding is significant as, despite the inherent differences between *in vivo* and *in vitro* systems (e.g., follicular microenvironment and monolayered culture plate vs. multilayered enclosed follicle), our hGLC model recapitulated the transcriptomic changes of numerous key ovulatory genes observed *in vivo*. Functional annotation and KEGG pathway analyses of hCG-upregulated genes further support this claim by highlighting enriched biological pathways associated with cholesterol biosynthesis/metabolism, steroid biosynthesis, cellular metabolism, cortisol synthesis and secretion, angiogenesis, glycolysis, MAPK signaling pathway, and HIF-1 signaling pathway (Table S5). Previous studies by our laboratory and others have demonstrated that these pathways are up-regulated by hCG and down-regulated by RU486 and implicated in functional changes associated with ovulation and luteinization.[11,17,34–38] Moreover, the IPA upstream regulator analysis further identified several enriched upstream transcriptional regulators for these genes, including PGR, FOS, CEBPB, SOX9, and KLF15, not only highlighting PGR as a core regulator of these genes but also identifying potential PGR co-transcriptional regulators involved in the ovulatory process. Together, these data strongly support the physiological relevance and validity of our model for studying PGR-mediated regulatory networks in humans.

While the identification of potential PGR-regulated genes by inhibiting PGR's action with RU486 in hGLCs has provided preliminary insight into the PGR-mediated ovulatory pathways in human preovulatory follicles, the dual antagonistic nature of RU486, which inhibits both PGR and NR3C1, presents challenges in distinguishing PGR-regulated genes from NR3C1-regulated genes. Particularly, recent studies have reported increases in cortisol levels and up-regulated expression of *NR3C1* in human preovulatory follicles as well as in hGLCs.[34,39–42] To address this concern, PGR-ChIP-seq analysis

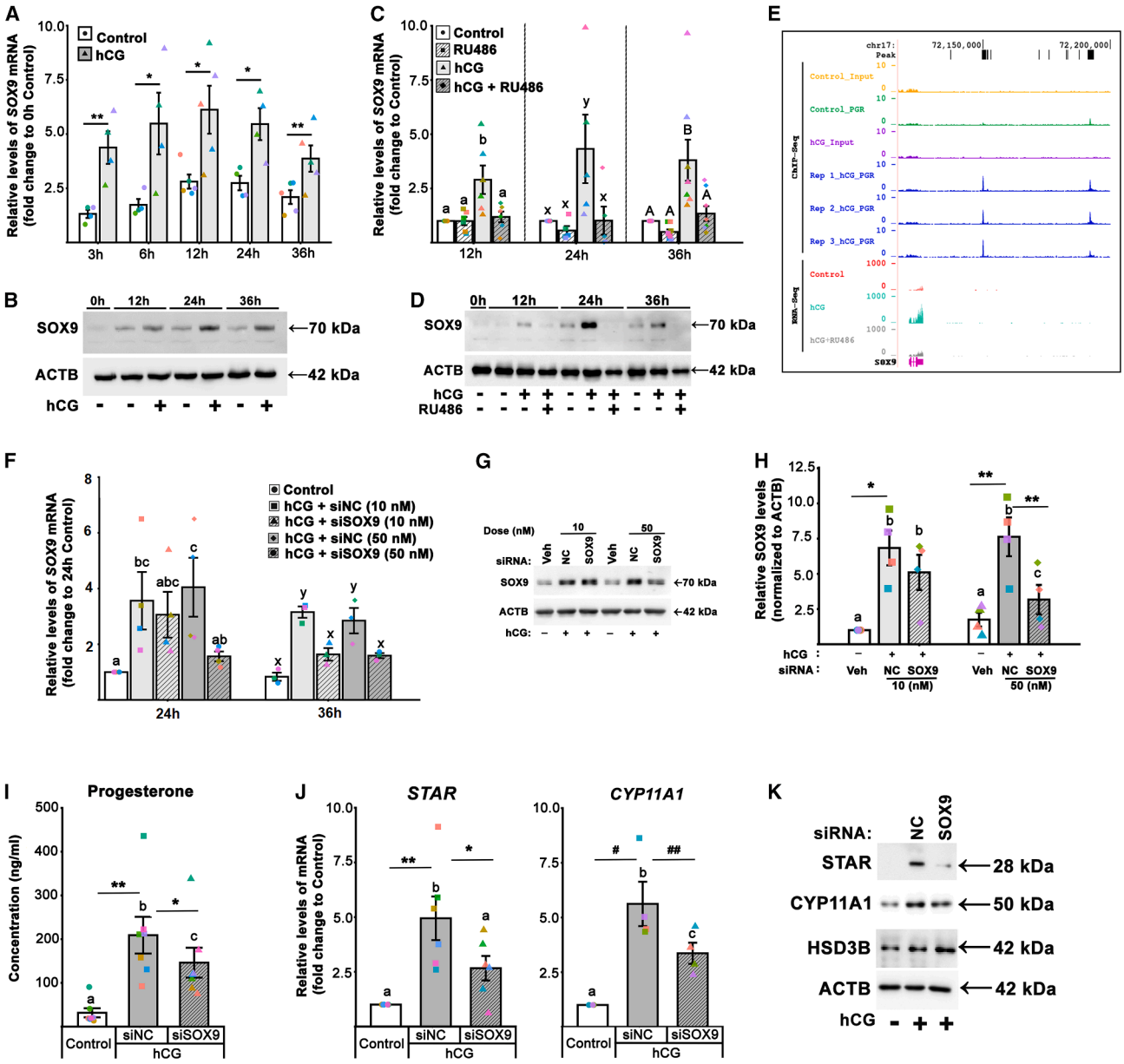

Figure 6. Regulation of *SOX9* expression by PGR and the role of SOX9 in progesterone production and the expression of steroidogenic factors in hGLCs

(A) hGLCs were treated without (control) or with hCG for various time points. *SOX9* mRNA levels were measured by qPCR and normalized to *GNPDA2* mRNA levels in each sample (n = 4–5 individual patient samples). *$0.01 \leq p < 0.05$. **$0.001 \leq p < 0.01$. Exact p values for control vs. hCG (3–36 h): 0.007, 0.026, 0.017, 0.012, 0.006 (paired t test).

(B) SOX9 was detected by western blot using whole-cell extracts from control or hCG-treated cells collected at various time points. The membrane was reprobed with an ACTB antibody to assess protein levels across all samples. The experiments were repeated three times, each with individual patient samples.

(C) hGLCs were treated with or without RU486 in the presence or absence of hCG for various time points. *SOX9* mRNA levels were measured by qPCR and normalized to *GNPDA2* mRNA levels in each sample (n = 3–7 individual patient samples). Bars without common superscripts are significantly different within each time point ($p < 0.05$; one-way ANOVA, followed by Duncan's test).

(D) Representative western blot showing SOX9 protein levels in whole-cell extracts. The membrane was reprobed for ACTB protein as a loading control. The experiments were repeated three times, each with individual patient samples.

(E) PGR-binding sites and gene expression levels on *SOX9* in hGLCs were visualized using the UCSC Genome Browser. Tracks 1 to 6 display PGR-binding peaks along the *SOX9* gene locus in hGLCs treated with or without hCG. Peak height represents binding intensity, and the input track serves as background noise control. Tracks 7 to 9 show RNA-seq read coverage across the *SOX9* exons under control, hCG, or hCG + RU486 treatments, with peak height reflecting expression levels.

(legend continued on next page)

was performed. Approximately 75% of the genes identified through RNA-seq were found to have PGR-binding sites on their promoters or in proximity, confirming the direct transcriptional regulatory role of PGR on these genes. These data not only confirmed our previous findings, which identified several genes listed[34] in Figure 3G, but also revealed a new list of genes that are direct downstream genes of PGR in hGLCs (Table S8). While some PGR-binding sites were enriched near TSSs, we also discovered PGR binding within introns, exons, and intergenic regions of the same genes. Gene expression is known to be regulated not only by promoters but also by distal regulatory elements such as enhancers, silencers, and insulators.[43] These distal PGR-binding sites may participate in long-range chromatin interactions or enhancer-mediated regulation.

For the remaining 25% of genes regulated by RU486 inhibition but not physically bound to PGR, their expression may be regulated by NR3C1 or other transcription factors downstream of PGR, such as FOS and SOX9. Consistent with this concept, a previous study showed that FOS regulates the expression of numerous genes in hGLCs.[33,35] Additionally, *de novo* motif analysis of ChIP-seq data detected AP-1 and SOX-binding motifs on PGR-bound DNA regions, suggesting that FOS and SOX9 not only act downstream of PGR-regulated genes but also work together with PGR to regulate the expression of crucial ovulatory and luteal genes. Among the transcriptional regulators newly identified to be regulated by PGR, SOX9 is particularly noteworthy, as its roles in ovarian function remain largely unstudied, warranting further investigation as a potential mediator of LH signaling in conjunction with PGR and other transcription factors during ovulation.

SOX9 is well known for its role in the gonadal sex determination in mammals.[29] In developing gonads, *Sox9* is initially expressed at a low level in both sexes but significantly increased by SRY (sex-determining region Y protein) in XY gonads, while it disappears or is repressed in XX gonads.[29] The active repression of *Sox9* expression in granulosa cells in the ovary is thought to be crucial for maintaining ovarian cell fate and phenotype.[30,31,44] Indeed, in the mouse ovary, SOX9 protein is absent in granulosa cells but only transiently expressed in non-steroidogenic cells in the theca layer.[45] Contradicting this report, our RNA-seq and ChIP-seq analyses indicate that *SOX9* is expressed in hGLCs and is regulated by the LH-PGR signaling pathway. Interestingly, in the long-term bovine granulosa cell cultures, *Sox9* expression was transiently increased and regulated by chemical inhibitors or activators of the specific signaling pathway.[46] However, it is not known whether *SOX9* is expressed *in vivo* in bovine granulosa cells of the follicle. Because our data on *SOX9* expressions were also obtained from primary human granulosa cell cultures, it was critically important to determine whether *SOX9* is truly expressed in granulosa cells of follicles *in vivo* in humans. Therefore, the present study characterized the *in vivo* expression of *SOX9* in dominant follicles from regularly cycling women: the mRNA levels were markedly elevated in early ovulatory follicles but returned to preovulatory levels in the late ovulatory phase. However, the increased SOX9 protein localization continued in late and post-ovulatory follicles, indicating that SOX9 plays a role in both ovulation and corpus luteum development in humans. Notably, SOX9 localization was predominantly observed in granulosa cells, which contrasts with its localization in non-steroidogenic theca cells in mice.[45] Another significant discovery of our study was the higher expression of *SOX9* in cumulus cells compared to granulosa cells immediately prior to ovulation at the time of oocyte retrieval. At present, the significance of higher expression level in cumulus compared to mural granulosa cells remains unclear and requires further investigation. One possibility is that the *SOX9* expression in cumulus cells contributes to local steroidogenesis, thereby supporting critical processes such as cumulus expansion, cumulus cell differentiation, and oocyte maturation. Together, these findings suggested the role of SOX9 in regulating the function of both granulosa cells and cumulus cells of human ovulatory follicles.

Indeed, a siRNA-mediated *SOX9* knockdown approach showed the role of SOX9 in hCG-induced progesterone production and the expression of steroidogenic genes, *STAR* and *CYP11A1*, shedding light on the role of SOX9 in regulating steroidogenesis during the periovulatory phase. Our findings are consistent with a previous report showing that targeted degradation of *SOX9* mRNA resulted in reduced expression of *STAR* and the levels of progesterone in bovine granulosa cells.[46]

(F) hGLCs were transfected with no siRNA (control), 10 or 50 nM of scrambled siRNA (negative control, siNC), or siRNA-targeting *SOX9* (siSOX9). After 3 h of transfection, the cells were cultured with or without hCG for an additional 24 or 36 h. The efficiency of *SOX9* knockdown was assessed by measuring *SOX9* mRNA levels using qPCR, with normalization to *GNPDA2* mRNA levels in each sample ($n = 4$ for 24 h; $n = 3$ for 36 h, using individual patient samples). Bars without common superscripts are significantly different within each time point ($p < 0.05$; one-way ANOVA, followed by paired two-tailed *t* test).

(G) Representative western blot showing SOX9 protein levels in whole-cell extracts isolated from hGLCs treated without (Veh) or with siNC or siSOX9 in the absence or presence of hCG. The membrane was reprobed for ACTB protein as a loading control.

(H) Densitometric quantification of SOX9 protein levels normalized to ACTB from 4 independent experiments, measured using ImageJ. Bars without common superscripts are significantly different ($p < 0.05$). Exact *p* values for indicated pairwise comparisons: $^{*}p = 0.018$. $^{**}p = 0.013$ (one-way ANOVA, followed by paired two-tailed *t* test).

(I) Progesterone levels in the conditioned media collected at 36 h from control, or hCG with siNC or siSOX9 at 50 nM were measured ($n = 7$ individual patient samples). Bars without common superscripts are significantly different ($p < 0.05$). The exact *p* values for the indicated pairwise comparisons: $^{*}p = 0.002$, $^{**}p = 0.004$ (one-way ANOVA, followed by paired two-tailed *t* test).

(J) The levels of mRNA for *STAR* and *CYP11A1* were measured by qPCR in samples collected at 36 h from control, or hCG with siNC or siSOX9 at 50 nM and normalized to the levels of *GNPDA2* mRNA ($n = 6$ for *STAR*; $n = 4$ for *CYP11A1*, using individual patient samples). Bars without common superscripts are significantly different ($p < 0.05$). The exact *p* values for the indicated pairwise comparisons: $^{*}p = 0.04$, $^{**}p = 0.01$, $\#p = 0.02$, $\#\#p = 0.048$ (one-way ANOVA, followed by paired two-tailed *t* test).

(K) STAR, CYP11A1, and HSD3B were detected by western blot using whole-cell extracts collected at 36 h from control, or hCG with siNC or siSOX9 at 50 nM. The membrane was reprobed for ACTB as a loading control. The experiments were repeated three times, each with individual patient samples. In all bar graphs, results are presented as the mean ± SEM. Each colored dot represents an individual patient, with the same color used across treatments or time points. hGLCs obtained from women undergoing *in vitro* fertilization were acclimated for 6 days.

Together, these findings imply that SOX9 is integral to regulating steroidogenesis in granulosa cells, mediating the effects of the LH-PGR signaling pathway on progesterone production.

Previous studies on the ovulatory process have frequently used mouse models, taking advantage of their physiological and hormonal similarities to humans in the ovulatory process, as well as their well-characterized genetic modifications and shorter reproductive cycles. Multiple *Pgr*KO mouse lines have been used to study the role of PGR in the ovulatory process, identifying its downstream target genes in preovulatory follicles.[9,14,26,27] Comparing previous mouse data to our findings from human data is crucial for identifying conserved regulatory mechanisms as well as species-specific differences, enhancing the accuracy of conclusions applicable to human biology and medicine. Comparative analyses of our datasets with those of Dinh et al. identified a shared set of genes, highlighting the conserved ovulatory pathway between these two species.[26] Notable RNA-seq overlaps included *VCAN/Vcan* and *SLCO2A1/Slco2a1*, genes involved in the stabilization of the cumulus oocyte complex (COC) matrix and proper COC expansion, both essential events during ovulation, highlighting their evolutionary significance in reproductive processes.[47] From ChIP-seq datasets, we identified additional conserved genes associated with diverse ovulatory roles, including oocyte maturation (*AREG*, *EREG*, and *EGFR*), COC expansion (*LYVE1* and *HAS2*), exocytosis (*SNAP25*), follicle rupture and oocytes release (*EDN2* and *PTGES*), CL formation (*RUNX1* and *RUNX2*), steroidogenesis (*STAR* and *CYP11A1*), and angiogenesis (*VEGFA*).[27,34,48–58] Our findings underscore the presence of conserved PGR-driven ovulatory pathways across species. Nevertheless, species-specific differences in gene regulation, such as those involving *SOX9*, emphasize the importance of cross-species studies to fully elucidate ovulatory mechanisms, as findings in animals may not always translate directly to human physiology.

In conclusion, our study demonstrates that PGR functions as a master coordinator of the ovulatory process and luteinization in the human ovary, directly regulating genes involved in transcriptional regulation, oocyte maturation, cumulus cell expansion, tissue remodeling, steroidogenesis, prostaglandin synthesis and transport, and angiogenesis. The identification of SOX9 as a new PGR downstream mediator, along with co-transcriptional regulators working in concert with PGR, reveals a complex transcriptional network governing hCG-induced and PGR-mediated ovulatory pathways. Furthermore, by delineating both conserved and species-specific PGR regulatory mechanisms, the present study not only identifies pathways that can be explored using mouse models but also underscores the critical importance of investigating the human-specific changes to fully elucidate the ovulatory process in humans. Considering the clinical use of PGR inhibitors, such as RU486 and ulipristal acetate, as emergency contraceptives due to their ability to delay or block ovulation,[19,59] our findings provide valuable insights into potential therapeutic targets for advancing the management of women's reproductive health.

Limitations of the study

While our *in vitro* model effectively recapitulates key aspects of *in vivo* physiology, it may not fully capture the complexity of *in vivo* regulation. Cell transfection methods, although useful for targeted gene manipulation, may not fully reflect the physiological cellular condition.

RESOURCE AVAILABILITY

Lead contact

Requests for further information, resources, and reagents should be directed to and will be fulfilled by the lead contact, Misung Jo (mjo2@uky.edu).

Materials availability

This study did not generate new unique reagents.

Data and code availability

- RNA-seq and ChIP-seq data generated in this study have been deposited in the NCBI Gene Expression Omnibus (GEO) repository and are publicly available as of the date of publication. Accession numbers GSE286909 (RNA-seq) and GSE286910 (PGR ChIP-seq) are listed in the key resources table. Previously published datasets analyzed in this study are available in GEO under accession numbers GSE168213 and GSE115820.
- New code is not generated for this study.
- Any additional information required to reanalyze the data reported in this paper is available from the lead contact upon request.

ACKNOWLEDGMENTS

This study was supported by P01HD71875, R01HD096077, R01HD116429, and R21HD119324 from the National Institutes of Health, United States, and the BTPSRF of the University of Kentucky Markey Cancer Center (P30CA177558).

AUTHOR CONTRIBUTIONS

Conceptualization, M.J. and H.J.; methodology, M.J. and H.J.; formal analysis, M.J. and H.J.; investigation, H.J. and Y.C.; resources, M.B., J.W.A., and T.E.C., Jr.; writing – original draft, M.J. and H.J.; writing – review and editing, M.J., H.J., Y.C., M.B., J.W.A., and T.E.C., Jr.; visualization, M.J. and H.J.; supervision, M.J.; funding acquisition, M.J., M.B., and T.E.C., Jr.

DECLARATION OF INTERESTS

The authors declare no competing interests.

STAR★METHODS

Detailed methods are provided in the online version of this paper and include the following:

- KEY RESOURCES TABLE
- EXPERIMENTAL MODEL AND STUDY PARTICIPANT DETAILS
  - Human granulosa/lutein cell Isolation and cultures
- METHOD DETAILS
  - RNA-sequencing
  - Chromatin immunoprecipitation (ChIP)-Sequencing
  - *SOX9* Silencing by small interfering RNA (siRNA)
  - Immunohistochemistry
  - Gene expression analysis
  - Western Blot analysis
  - Progesterone assay
- QUANTIFICATION AND STATISTICAL ANALYSIS

SUPPLEMENTAL INFORMATION

Supplemental information can be found online at https://doi.org/10.1016/j.isci.2026.116044.

Received: March 26, 2025
Revised: September 19, 2025
Accepted: May 5, 2026

REFERENCES

1. Holesh, J.E., Bass, A.N., and Lord, M. (2024). Physiology, Ovulation (StatPearls).
2. Richards, J.S., and Pangas, S.A. (2010). The ovary: basic biology and clinical implications. J. Clin. Investig. *120*, 963–972. https://doi.org/10.1172/JCI41350.
3. Espey, L.L., Richards, J., and Neill, J. (1994). Physiology of Reproduction (New York: Raven Press).
4. Lydon, J.P., DeMayo, F.J., Funk, C.R., Mani, S.K., Hughes, A.R., Montgomery, C.A., Jr., Shyamala, G., Conneely, O.M., and O'Malley, B.W. (1995). Mice lacking progesterone receptor exhibit pleiotropic reproductive abnormalities. Genes Dev. *9*, 2266–2278. https://doi.org/10.1101/gad.9.18.2266.
5. Akison, L.K., and Robker, R.L. (2012). The critical roles of progesterone receptor (PGR) in ovulation, oocyte developmental competence and oviductal transport in mammalian reproduction. Reprod. Domest. Anim. *47*, 288–296. https://doi.org/10.1111/j.1439-0531.2012.02088.x.
6. Grimm, S.L., Hartig, S.M., and Edwards, D.P. (2016). Progesterone Receptor Signaling Mechanisms. J. Mol. Biol. *428*, 3831–3849. https://doi.org/10.1016/j.jmb.2016.06.020.
7. Joshi, H., and Press, M.F. (2018). 22 - Molecular Oncology of Breast Cancer. In The Breast, Fifth Edition, K.I. Bland, E.M. Copeland, V.S. Klimberg, and W.J. Gradishar, eds. (Elsevier), pp. 282–307.e285. https://doi.org/10.1016/B978-0-323-35955-9.00022-2.
8. Choi, Y., Wilson, K., Hannon, P.R., Rosewell, K.L., Brannstrom, M., Akin, J.W., Curry, T.E., Jr., and Jo, M. (2017). Coordinated Regulation Among Progesterone, Prostaglandins, and EGF-Like Factors in Human Ovulatory Follicles. J. Clin. Endocrinol. Metab. *102*, 1971–1982. https://doi.org/10.1210/jc.2016-3153.
9. Robker, R.L., Russell, D.L., Espey, L.L., Lydon, J.P., O'Malley, B.W., and Richards, J.S. (2000). Progesterone-regulated genes in the ovulation process: ADAMTS-1 and cathepsin L proteases. Proc. Natl. Acad. Sci. USA *97*, 4689–4694. https://doi.org/10.1073/pnas.080073497.
10. Park, O.K., and Mayo, K.E. (1991). Transient expression of progesterone receptor messenger RNA in ovarian granulosa cells after the preovulatory luteinizing hormone surge. Mol. Endocrinol. *5*, 967–978. https://doi.org/10.1210/mend-5-7-967.
11. Duffy, D.M., Ko, C., Jo, M., Brannstrom, M., and Curry, T.E. (2019). Ovulation: Parallels With Inflammatory Processes. Endocr. Rev. *40*, 369–416. https://doi.org/10.1210/er.2018-00075.
12. Clemens, J.W., Robker, R.L., Kraus, W.L., Katzenellenbogen, B.S., and Richards, J.S. (1998). Hormone induction of progesterone receptor (PR) messenger ribonucleic acid and activation of PR promoter regions in ovarian granulosa cells: evidence for a role of cyclic adenosine 3',5'-monophosphate but not estradiol. Mol. Endocrinol. *12*, 1201–1214. https://doi.org/10.1210/mend.12.8.0157.
13. Natraj, U., and Richards, J.S. (1993). Hormonal regulation, localization, and functional activity of the progesterone receptor in granulosa cells of rat preovulatory follicles. Endocrinology *133*, 761–769. https://doi.org/10.1210/endo.133.2.8344215.
14. Smith, K.M., Dinh, D.T., Akison, L.K., Nicholls, M., Dunning, K.R., Morimoto, A., Lydon, J.P., Russell, D.L., and Robker, R.L. (2022). Intraovarian, Isoform-Specific Transcriptional Roles of Progesterone Receptor in Ovulation. Cells *11*, 1563. https://doi.org/10.3390/cells11091563.
15. Jo, M., Komar, C.M., and Fortune, J.E. (2002). Gonadotropin surge induces two separate increases in messenger RNA for progesterone receptor in bovine preovulatory follicles. Biol. Reprod. *67*, 1981–1988. https://doi.org/10.1095/biolreprod.102.004366.
16. Chaffin, C.L., Stouffer, R.L., and Duffy, D.M. (1999). Gonadotropin and steroid regulation of steroid receptor and aryl hydrocarbon receptor messenger ribonucleic acid in macaque granulosa cells during the periovulatory interval. Endocrinology *140*, 4753–4760. https://doi.org/10.1210/endo.140.10.7056.
17. Loutradis, D., Bletsa, R., Aravantinos, L., Kallianidis, K., Michalas, S., and Psychoyos, A. (1991). Preovulatory effects of the progesterone antagonist mifepristone (RU486) in mice. Hum. Reprod. *6*, 1238–1240. https://doi.org/10.1093/oxfordjournals.humrep.a137519.
18. Palanisamy, G.S., Cheon, Y.P., Kim, J., Kannan, A., Li, Q., Sato, M., Mantena, S.R., Sitruk-Ware, R.L., Bagchi, M.K., and Bagchi, I.C. (2006). A novel pathway involving progesterone receptor, endothelin-2, and endothelin receptor B controls ovulation in mice. Mol. Endocrinol. *20*, 2784–2795. https://doi.org/10.1210/me.2006-0093.
19. Ledger, W.L., Sweeting, V.M., Hillier, H., and Baird, D.T. (1992). Inhibition of ovulation by low-dose mifepristone (RU 486). Hum. Reprod. *7*, 945–950. https://doi.org/10.1093/oxfordjournals.humrep.a137776.
20. Brannstrom, M. (1993). Inhibitory effect of mifepristone (RU 486) on ovulation in the isolated perfused rat ovary. Contraception *48*, 393–402. https://doi.org/10.1016/0010-7824(93)90084-k.
21. Bishop, C.V., Hennebold, J.D., Kahl, C.A., and Stouffer, R.L. (2016). Knockdown of Progesterone Receptor (PGR) in Macaque Granulosa Cells Disrupts Ovulation and Progesterone Production. Biol. Reprod. *94*, 109. https://doi.org/10.1095/biolreprod.115.134981.
22. Mishra, B., Park, J.Y., Wilson, K., and Jo, M. (2015). X-linked lymphocyte regulated gene 5c-like (Xlr5c-like) is a novel target of progesterone action in granulosa cells of periovulatory rat ovaries. Mol. Cell. Endocrinol. *412*, 226–238. https://doi.org/10.1016/j.mce.2015.05.008.
23. Li, F., Liu, J., Jo, M., and Curry, T.E., Jr. (2011). A role for nuclear factor interleukin-3 (NFIL3), a critical transcriptional repressor, in down-regulation of periovulatory gene expression. Mol. Endocrinol. *25*, 445–459. https://doi.org/10.1210/me.2010-0250.
24. Sayasith, K., and Sirois, J. (2014). Expression and regulation of stromal cell-derived factor-1 (SDF1) and chemokine CXC motif receptor 4 (CXCR4) in equine and bovine preovulatory follicles. Mol. Cell. Endocrinol. *391*, 10–21. https://doi.org/10.1016/j.mce.2014.04.009.
25. Dinh, D.T., Breen, J., Akison, L.K., DeMayo, F.J., Brown, H.M., Robker, R.L., and Russell, D.L. (2019). Tissue-specific progesterone receptor-chromatin binding and the regulation of progesterone-dependent gene expression. Sci. Rep. *9*, 11966. https://doi.org/10.1038/s41598-019-48333-8.
26. Dinh, D.T., Breen, J., Nicol, B., Foot, N.J., Bersten, D.C., Emery, A., Smith, K.M., Wong, Y.Y., Barry, S.C., Yao, H.H.C., et al. (2023). Progesterone receptor mediates ovulatory transcription through RUNX transcription factor interactions and chromatin remodelling. Nucleic Acids Res. *51*, 5981–5996. https://doi.org/10.1093/nar/gkad271.
27. Park, C.J., Lin, P.C., Zhou, S., Barakat, R., Bashir, S.T., Choi, J.M., Cacioppo, J.A., Oakley, O.R., Duffy, D.M., Lydon, J.P., and Ko, C.J. (2020). Progesterone Receptor Serves the Ovary as a Trigger of Ovulation and a Terminator of Inflammation. Cell Rep. *31*, 107496. https://doi.org/10.1016/j.celrep.2020.03.060.
28. Al-Alem, L., Puttabyatappa, M., Rosewell, K., Brannstrom, M., Akin, J., Boldt, J., Muse, K., and Curry, T.E., Jr. (2015). Chemokine Ligand 20: A Signal for Leukocyte Recruitment During Human Ovulation? Endocrinology *156*, 3358–3369. https://doi.org/10.1210/en.2014-1874.
29. Gonen, N., and Lovell-Badge, R. (2019). The regulation of Sox9 expression in the gonad. Curr. Top. Dev. Biol. *134*, 223–252. https://doi.org/10.1016/bs.ctdb.2019.01.004.
30. Lindeman, R.E., Gearhart, M.D., Minkina, A., Krentz, A.D., Bardwell, V.J., and Zarkower, D. (2015). Sexual cell-fate reprogramming in the ovary by DMRT1. Curr. Biol. *25*, 764–771. https://doi.org/10.1016/j.cub.2015.01.034.
31. Zhao, L., Svingen, T., Ng, E.T., and Koopman, P. (2015). Female-to-male sex reversal in mice caused by transgenic overexpression of Dmrt1. Development *142*, 1083–1088. https://doi.org/10.1242/dev.122184.

32. Poulsen, L.C., Botkjaer, J.A., Ostrup, O., Petersen, K.B., Andersen, C.Y., Grondahl, M.L., and Englund, A.L.M. (2020). Two waves of transcriptomic changes in periovulatory human granulosa cells. Hum. Reprod. *35*, 1230–1245. https://doi.org/10.1093/humrep/deaa043.

33. Choi, Y., Rosewell, K.L., Brannstrom, M., Akin, J.W., Curry, T.E., Jr., and Jo, M. (2018). FOS, a Critical Downstream Mediator of PGR and EGF Signaling Necessary for Ovulatory Prostaglandins in the Human Ovary. J. Clin. Endocrinol. Metab. *103*, 4241–4252. https://doi.org/10.1210/jc.2017-02532.

34. Jeon, H., Choi, Y., Brannstrom, M., Akin, J.W., Curry, T.E., and Jo, M. (2023). Cortisol/glucocorticoid receptor: a critical mediator of the ovulatory process and luteinization in human periovulatory follicles. Hum. Reprod. *38*, 671–685. https://doi.org/10.1093/humrep/dead017.

35. Choi, Y., Jeon, H., Akin, J.W., Curry, T.E., and Jo, M. (2021). The FOS/AP-1 Regulates Metabolic Changes and Cholesterol Synthesis in Human Periovulatory Granulosa Cells. Endocrinology *162*, bqab127. https://doi.org/10.1210/endocr/bqab127.

36. Mauro, A., Berardinelli, P., Russo, V., Bernabo, N., Martelli, A., Nardinocchi, D., Di Giacinto, O., Turriani, M., and Barboni, B. (2021). Effects of P(4) Antagonist RU486 on VEGF and Its Receptors' Signaling during the In Vivo Transition from the Preovulatory to Periovulatory Phase of Ovarian Follicles. Int. J. Mol. Sci. *22*, 13520. https://doi.org/10.3390/ijms222413520.

37. Tanaka, N., Iwamasa, J., Matsuura, K., and Okamura, H. (1993). Effects of progesterone and anti-progesterone RU486 on ovarian 3 beta-hydroxysteroid dehydrogenase activity during ovulation in the gonadotrophin-primed immature rat. J. Reprod. Fertil. *97*, 167–172. https://doi.org/10.1530/jrf.0.0970167.

38. Kawano, T., Okamura, H., Tajima, C., Fukuma, K., and Katabuchi, H. (1988). Effect of RU 486 on luteal function in the early pregnant rat. J. Reprod. Fertil. *83*, 279–285. https://doi.org/10.1530/jrf.0.0830279.

39. Yong, P.Y., Thong, K.J., Andrew, R., Walker, B.R., and Hillier, S.G. (2000). Development-related increase in cortisol biosynthesis by human granulosa cells. J. Clin. Endocrinol. Metab. *85*, 4728–4733. https://doi.org/10.1210/jcem.85.12.7005.

40. Fateh, M., Ben-Rafael, Z., Benadiva, C.A., Mastroianni, L., Jr., and Flickinger, G.L. (1989). Cortisol levels in human follicular fluid. Fertil. Steril. *51*, 538–541. https://doi.org/10.1016/s0015-0282(16)60572-1.

41. Lewicka, S., von Hagens, C., Hettinger, U., Grunwald, K., Vecsei, P., Runnebaum, B., and Rabe, T. (2003). Cortisol and cortisone in human follicular fluid and serum and the outcome of IVF treatment. Hum. Reprod. *18*, 1613–1617. https://doi.org/10.1093/humrep/deg352.

42. Andersen, C.Y., Morineau, G., Fukuda, M., Westergaard, L.G., Ingerslev, H.J., Fiet, J., and Byskov, A.G. (1999). Assessment of the follicular cortisol:cortisone ratio. Hum. Reprod. *14*, 1563–1568. https://doi.org/10.1093/humrep/14.6.1563.

43. Spitz, F., and Furlong, E.E. (2012). Transcription factors: from enhancer binding to developmental control. Nat. Rev. Genet. *13*, 613–626. https://doi.org/10.1038/nrg3207.

44. Uhlenhaut, N.H., Jakob, S., Anlag, K., Eisenberger, T., Sekido, R., Kress, J., Treier, A.C., Klugmann, C., Klasen, C., Holter, N.I., et al. (2009). Somatic sex reprogramming of adult ovaries to testes by FOXL2 ablation. Cell *139*, 1130–1142. https://doi.org/10.1016/j.cell.2009.11.021.

45. Notarnicola, C., Malki, S., Berta, P., Poulat, F., and Boizet-Bonhoure, B. (2006). Transient expression of SOX9 protein during follicular development in the adult mouse ovary. Gene Expr. Patterns *6*, 695–702. https://doi.org/10.1016/j.modgep.2006.01.001.

46. Baddela, V.S., Michaelis, M., Tao, X., Koczan, D., and Vanselow, J. (2023). ERK1/2-SOX9/FOXL2 axis regulates ovarian steroidogenesis and favors the follicular-luteal transition. Life Sci. Alliance *6*. https://doi.org/10.26508/lsa.202302100.

47. Richards, J.S., Russell, D.L., Ochsner, S., and Espey, L.L. (2002). Ovulation: new dimensions and new regulators of the inflammatory-like response. Annu. Rev. Physiol. *64*, 69–92. https://doi.org/10.1146/annurev.physiol.64.081501.131029.

48. Reizel, Y., Elbaz, J., and Dekel, N. (2010). Sustained activity of the EGF receptor is an absolute requisite for LH-induced oocyte maturation and cumulus expansion. Mol. Endocrinol. *24*, 402–411. https://doi.org/10.1210/me.2009-0267.

49. Hsieh, M., Thao, K., and Conti, M. (2011). Genetic dissection of epidermal growth factor receptor signaling during luteinizing hormone-induced oocyte maturation. PLoS One *6*, e21574. https://doi.org/10.1371/journal.pone.0021574.

50. Shimada, M., Hernandez-Gonzalez, I., Gonzalez-Robayna, I., and Richards, J.S. (2006). Paracrine and autocrine regulation of epidermal growth factor-like factors in cumulus oocyte complexes and granulosa cells: key roles for prostaglandin synthase 2 and progesterone receptor. Mol. Endocrinol. *20*, 1352–1365. https://doi.org/10.1210/me.2005-0504.

51. Johnson, L.A., Prevo, R., Clasper, S., and Jackson, D.G. (2007). Inflammation-induced uptake and degradation of the lymphatic endothelial hyaluronan receptor LYVE-1. J. Biol. Chem. *282*, 33671–33680. https://doi.org/10.1074/jbc.M702889200.

52. Prevo, R., Banerji, S., Ferguson, D.J., Clasper, S., and Jackson, D.G. (2001). Mouse LYVE-1 is an endocytic receptor for hyaluronan in lymphatic endothelium. J. Biol. Chem. *276*, 19420–19430. https://doi.org/10.1074/jbc.M011004200.

53. Shimada, M., Yanai, Y., Okazaki, T., Yamashita, Y., Sriraman, V., Wilson, M.C., and Richards, J.S. (2007). Synaptosomal-associated protein 25 gene expression is hormonally regulated during ovulation and is involved in cytokine/chemokine exocytosis from granulosa cells. Mol. Endocrinol. *21*, 2487–2502. https://doi.org/10.1210/me.2007-0042.

54. Ko, C., Gieske, M.C., Al-Alem, L., Hahn, Y., Su, W., Gong, M.C., Iglarz, M., and Koo, Y. (2006). Endothelin-2 in ovarian follicle rupture. Endocrinology *147*, 1770–1779. https://doi.org/10.1210/en.2005-1228.

55. Park, E.S., Lind, A.K., Dahm-Kahler, P., Brannstrom, M., Carletti, M.Z., Christenson, L.K., Curry, T.E., Jr., and Jo, M. (2010). RUNX2 transcription factor regulates gene expression in luteinizing granulosa cells of rat ovaries. Mol. Endocrinol. *24*, 846–858. https://doi.org/10.1210/me.2009-0392.

56. Park, E.S., Park, J., Franceschi, R.T., and Jo, M. (2012). The role for runt related transcription factor 2 (RUNX2) as a transcriptional repressor in luteinizing granulosa cells. Mol. Cell. Endocrinol. *362*, 165–175. https://doi.org/10.1016/j.mce.2012.06.005.

57. Jo, M., and Curry, T.E., Jr. (2006). Luteinizing hormone-induced RUNX1 regulates the expression of genes in granulosa cells of rat periovulatory follicles. Mol. Endocrinol. *20*, 2156–2172. https://doi.org/10.1210/me.2005-0512.

58. Coultas, L., Chawengsaksophak, K., and Rossant, J. (2005). Endothelial cells and VEGF in vascular development. Nature *438*, 937–945. https://doi.org/10.1038/nature04479.

59. Rosato, E., Farris, M., and Bastianelli, C. (2015). Mechanism of Action of Ulipristal Acetate for Emergency Contraception: A Systematic Review. Front. Pharmacol. *6*, 315. https://doi.org/10.3389/fphar.2015.00315.

60. Ewels, P.A., Peltzer, A., Fillinger, S., Patel, H., Alneberg, J., Wilm, A., Garcia, M.U., Di Tommaso, P., and Nahnsen, S. (2020). The nf-core framework for community-curated bioinformatics pipelines. Nat. Biotechnol. *38*, 276–278. https://doi.org/10.1038/s41587-020-0439-x.

61. Law, C.W., Alhamdoosh, M., Su, S., Dong, X., Tian, L., Smyth, G.K., and Ritchie, M.E. (2016). RNA-seq analysis is easy as 1-2-3 with limma, Glimma and edgeR. F1000Res. *5*. https://doi.org/10.12688/f1000research.9005.3.

62. Jo, M., Brannstrom, M., Akins, J.W., and Curry, T.E., Jr. (2025). New insights into the ovulatory process in the human ovary. Hum. Reprod. Update *31*, 21–47. https://doi.org/10.1093/humupd/dmae027.

63. Pfaffl, M.W. (2001). A new mathematical model for relative quantification in real-time RT-PCR. Nucleic Acids Res. *29*, e45. https://doi.org/10.1093/nar/29.9.e45.

STAR★METHODS

KEY RESOURCES TABLE

REAGENT or RESOURCE	SOURCE	IDENTIFIER
Antibodies		
PGR	Cell Signaling Technology	Cat#8757; RRID: AB_2797144
SOX9	Cell Signaling Technology	Cat# 82630; RRID: AB_2665492
STAR	Cell Signaling Technology	Cat#8449
CYP11A1	Cell Signaling Technology	Cat#14217
HSD3B	Santa Cruz Biotechnology	Cat#sc-30820
ACTB	Santa Cruz Biotechnology	Cat#sc-47778
Anti-rabbit IgG, HRP-linked Antibody	Cell Signaling Technology	Cat # 7074
bovine anti-goat IgG-HRP	Santa Cruz Biotechnology	Cat#sc-2378
Biological samples		
Human follicular aspirates	Bluegrass Fertility Center	N/A
Human follicular tissues	Sahlgrenska University Hospital	N/A
Chemicals, peptides, and recombinant proteins		
RU486	Cayman Chemical	Cat# 10006317
hCG	Sigma-Aldrich	Cat# CG10
SuperScript IV	Invitrogen Life Technologies	Cat# 18090200
RNaseOUT	Invitrogen Life Technologies	Cat# 10777019
OptiMEM medium	Gibco	Cat# 31985062
Lipofectamine RNAiMAX	Thermo Fisher Scientific	Cat# 13778150
ImmPRESS-AP Horse Anti-Rabbit IgG Polymer Detection Kit	Vector Laboratories	Cat# MP-5401
Brilliant III Ultra-Fast SYBR Green	Agilent Technologies	Cat# 600884
ImmPACT Vector Red	Vector Laboratories	Cat# SK-5105
TaqMan Fast Advanced Master Mix	Applied Biosystems	Cat# 4444963
Critical commercial assays		
RNeasy Mini Kit	Qiagen	Cat#74106
TruSeq Stranded mRNA Library Prep Kit	Illumina	Cat# RS-122-2103
NovaSeq S2 reagent kit	Illumina	Cat# 20012862
ChIP-IT High Sensitivity Kit	Active Motif	Cat# 53040
UltraLow System V2 DNA-Seq Library Preparation Kit	Tecan	Cat# 0344NB-96
NovaSeq X Series Reagent Kits v1.0	Illumina	Cat# 20085594
IMMULITE Progesterone Assay Kit	Siemens Healthineers	Cat# L2KPW2
Deposited data		
GEO dataset GSE168213	NCBI GEO	https://www.ncbi.nlm.nih.gov/geo/query/acc.cgi?acc=GSE168213
GEO dataset GSE115820	NCBI GEO	https://www.ncbi.nlm.nih.gov/geo/query/acc.cgi?acc=GSE115820
GEO dataset GSE286909	NCBI GEO	https://www.ncbi.nlm.nih.gov/geo/query/acc.cgi?acc=GSE286909
GEO dataset GSE286910	NCBI GEO	https://www.ncbi.nlm.nih.gov/geo/query/acc.cgi?acc=GSE286910
Experimental models: Organisms/strains		
Primary human granulosa/lutein cells	This study	N/A

(*Continued on next page*)

Continued

REAGENT or RESOURCE	SOURCE	IDENTIFIER
Oligonucleotides		
SOX9	Invitrogen Life Technologies	TaqMan primer (Hs00165814_m1)
GAPDH	Invitrogen Life Technologies	TaqMan primer (Hs00266705_g1)
STAR	Eurofins Genomics	(Foward ACGTGGATTAACCAGGTTCG, Reverse CAGCCCTCTTGGTTGCTAAG)
CYP11A1	Eurofins Genomics	Foward AGACGGGCACACACAAAGTC Reverse AGGCTGCCGACTTCTTCAACA
GNPDA2	Eurofins Genomics	Foward GTGCGTCACCGTAATGAGGC Reverse AGGTGTACTCCCTGTTGGTAAAC
SOX9 siRNA	Thermo Fisher Scientific	Assay ID s13306
Oligo (dT)20 primer	Integrated DNA Technologies	Custom oligonucleotide
Random Hexamer	Integrated DNA Technologies	Custom oligonucleotide
Software and algorithms		
R (v4.4.2)	R Foundation	https://www.r-project.org/
IBM SPSS (v.27)	IBM	https://www.ibm.com/products/spss-statistics; RRID: SCR_019096
nf-core/rnaseq pipeline	Ewels et al.[60]	https://nf-co.re/rnaseq
nf-core/chipseq pipeline	Ewels et al.[60]	https://nf-co.re/chipseq
bcl2fastq v2.20	Illumina	https://support.illumina.com
Ingenuity Pathway Analysis (IPA)	QIAGEN	RRID: SCR_008653
UCSC Genome Browser	UCSC	https://genome.ucsc.edu/
ImageJ v1.51	National Institutes of Health	https://imagej.net
DAVID	NIH	https://david.ncifcrf.gov/
Primer3	Primer3 developers	https://primer3.ut.ee/;RRID: SCR_003139
Primer-BLAST	NCBI	https://www.ncbi.nlm.nih.gov/tools/primer-blast/; RRID: SCR_003095
edgeR	Law et al.[61]	https://bioconductor.org/packages/edgeR; RRID: SCR_012802

EXPERIMENTAL MODEL AND STUDY PARTICIPANT DETAILS

The protocol using human tissues obtained *in vivo* was approved by the Human Ethics Committee of the Sahlgrenska Academy at the University of Gothenburg (Gothenburg, Sweden) (Dnr#732-10). Sample collection was conducted at the Division of Gynecology and Reproductive Medicine, Sahlgrenska University Hospital, and all participants provided written informed consent prior to participation. All participants met the following criteria: were healthy 30-to-38-year-old women undergoing laparoscopic sterilization, had exhibited regular menstrual cycles, and had not taken any hormonal contraceptives for at least 3 months before their enrollment in the study, as previously described.[28,62] Women were monitored by transvaginal ultrasound for two to three menstrual cycles before surgery to ascertain the occurrence of regular cycles and to monitor the growth of a dominant follicle during the follicular phase.[62] For patients undergoing tubal ligation for sterilization, the entire dominant follicle was collected by laparoscopic excision at the time points described in the following sections.

Patients were assigned to four groups based on ovulatory stage: pre-, early, late, and post-ovulatory phases. In the preovulatory group, surgery was performed when the follicle reached a diameter between 14 and 17.5 mm before the endogenous LH surge. These patients were not administered with hCG. The remaining women were given recombinant hCG via subcutaneous injection (10,000 IU, Ovitrelle; Merck, Darmstadt, Germany) and were divided into three groups: early ovulatory (surgery between 12 and 18 h post-hCG), late ovulatory (surgery between 18 and 34 h post-hCG), and post-ovulatory (between 44 and 70 h post-hCG) phase. To confirm that these patients exhibited a normal hormonal pattern before the LH surge or after hCG administration, blood samples were collected at the time of surgery and measured for serum progesterone and estradiol levels. Patient characteristics detailed in Table S1 were previously reported.[28]

The whole intact follicle was excised using laparoscopic scissors and then processed either for immunohistochemistry by fixing the whole follicle or for gene expression analysis by bisecting the follicle.[62] When the follicle was bisected, mural granulosa cells were

gently scraped from the interior using small tissue forceps. The follicular fluid and cell suspension were combined and centrifuged at 500 × *g* to pellet and collect the granulosa cells. The collected granulosa cells were frozen for subsequent experiments.

Human granulosa/lutein cell Isolation and cultures

Human granulosa/lutein cells (hGLCs) were obtained from aspirates of women undergoing *in vitro* fertilization (IVF). The collection protocol was approved by the Institutional Review Board of the University of Kentucky Office of Research Integrity (IRB #44977). Ovarian stimulation was achieved using individualized doses of recombinant human follicle-stimulating hormone (FSH) administered to patients at the Bluegrass Fertility Center (Lexington, KY, USA). After 9 to 11 days of FSH administration, patients received an injection of 10,000 IU of human chorionic gonadotropin (hCG), and the dominant follicles were aspirated 36 h later. The retrieved oocytes were used for the IVF process, and the remaining cumulus cells and hGLCs were collected for further analysis. The procedure for handling hGLCs followed the methods described previously.[8,28] Immediately after retrieval of the cumulus-oocyte complexes, the residual cells in the aspirates were subjected to 40% Percoll gradient centrifugation to remove red blood cells. The isolated cells were examined under a microscope to assess their morphology and were counted. They were then resuspended in an OptiMEM medium (Gibco; Waltham, Massachusetts, USA) supplemented with 10% fetal bovine serum and antibiotic-antimycotic and cultured on plates at a density of 2.5×10^5 cells/mL. The cells were acclimated for 6 days, changing media every 24 h to regain responsiveness to hCG. After the acclimation period, cells were serum-starved for 1 h and then subjected to various treatments in an OptiMEM medium supplemented with antibiotic-antimycotic. Treatments were carried out for the stated hours. All study participants were female; therefore, sex-based differences were not evaluated. Primary human granulosa/lutein cells were not subjected to cell line authentication. Cells were routinely monitored and were negative for mycoplasma contamination. All procedures were conducted in accordance with institutional guidelines and applicable regulations.

METHOD DETAILS

RNA-sequencing

Primary hGLCs obtained from IVF patients were treated with or without RU486 (20 μM) in the presence or absence of hCG (1 IU/mL) for 12 h. For each treatment, samples were collected from four individual patients, with each patient's sample used across all treatments to ensure paired comparison among treatments. Total RNA was extracted from hGLCs using the RNeasy Mini Kit (Qiagen; Hilden, Germany) and treated with DNase I. The integrity of RNA was assessed using a NanoDrop and electrophoresis. The isolated RNA was then utilized for library construction and sequencing at the Roy J. Carver Biotechnology Center at the University of Illinois Urbana-Champaign. Libraries were prepared using the TruSeq Stranded mRNA Library Prep Kit (Illumina; San Diego, CA, USA). The libraries were quantitated by qPCR and sequenced on a single lane for 101 cycles from one end of the fragments on a NovaSeq 6000 with a NovaSeq S2 reagent kit (Illumina). RNA-seq data were processed using the nf-core/rnaseq pipeline (v3.14.0) with default parameters.[60] Briefly, FASTQ files were generated and demultiplexed with the bcl2fastq v2.20 Conversion Software (Illumina). Adaptors were trimmed from the 3′ end of the reads, resulting in 2,332,045,900 filtered reads. Trimmed reads were aligned to the human genome version of GRCh38 from NCBI using STAR (2.7.10a) and SAMtools, and transcript levels were then quantified using Salmon (1.10.1). Differential gene expression analysis was performed using the Limma-trend method on edgeR package,[61] and differentially expressed genes (DEGs) for each treatment were defined as having a fold change $\geq |1.5|$ ($|\log_2 FC| \geq 0.5$) and a False-Discovery Rate (FDR) adjusted *p*-value <0.05. Upstream regulators of DEGs were assessed using Ingenuity Pathway Analysis (IPA) software (-QIAGEN; RRID: SCR_008653). To visualize RNA-Seq data on the UCSC Genome Browser (RRID: SCR_005780), read coverage was processed using BEDTools (2.30.0). Further analyses, including KEGG pathways and Gene Ontology (GO) enrichment, were performed with DAVID (RRID: SCR_001881).

RNA-Seq data on *Pgr*KO mouse granulosa cells collected at 8 h post-hCG were obtained from the publicly available database GEO: GSE168213.[26]

Chromatin immunoprecipitation (ChIP)-Sequencing

Primary hGLCs obtained from IVF patients were treated with or without hCG (1 IU/mL) for 12 h. The experimental design included one biological replicate for the control group and three biological replicates for the hCG-treated group, each containing at least 1×10^7 cells. ChIP experiments were performed using the ChIP-IT High Sensitivity Kit (Active Motif; Carlsbad, CA, USA) according to the manufacturer's protocol. Briefly, chromatin was extracted from cells fixed with 1.1% formaldehyde and fragmented using sonication. Sonicated chromatin (at least 10 mg per replicate) was immunoprecipitated with PGR antibody. The antibody-chromatin complexes were captured using Protein G agarose beads and eluted. Following elution, the crosslinks were reversed and purified. Libraries of purified DNA from ChIP and input samples were prepared with the UltraLow System V2 DNA-Seq Library Preparation Kit (Tecan; Durham, NC, USA). The libraries were pooled and quantitated by qPCR and sequenced on one 10B lane for 101 cycles from one end of the fragments on a NovaSeq X Plus with V1.0 sequenced kits (Illumina). ChIP-seq data were processed using the nf-core/chipseq pipeline (v2.0.0) with default parameters. Briefly, FASTQ files were generated and demultiplexed with the bcl2fastq v2.20 Conversion Software (Illumina). Adaptors have been trimmed from the 3′ end of the reads, resulting in 760,113,797 filtered reads. Trimmed reads were aligned to the human genome version of GRCh38 from NCBI using BWA (0.7.17-r1188). Peak calling was performed with MACS2 (vers. 2.2.7.1; RRID: SCR_013291) using default settings and input DNA as a control to identify regions of

enriched binding. For the hCG-treated group, peaks from three replicates were merged using MACS2 Consensus to obtain a consensus set of peaks. Overlapped peaks were used for all subsequent comparisons. Peaks were annotated, and motif analysis was conducted using HOMER (vers, 4.11; RRID: SCR_010881). Additional analyses, including KEGG pathways and GO enrichment, were performed using DAVID.

ChIP-Seq data for PGR in mouse granulosa cells were obtained from the publicly available database (GEO: GSE115820)[25] and analyzed as described above.

SOX9 Silencing by small interfering RNA (siRNA)

Primary hGLCs were transfected with siRNA targeting *SOX9* (Assay ID s13306, Thermo Fisher Scientific) or with scrambled siRNA (Negative Control) using Lipofectamine RNAiMAX Transfection Reagent, following the manufacturer's protocol for 3 h. The cells were then stimulated with hCG (1 IU/mL) and cultured for an additional 24 h or 36 h. The conditioned media and the cells were used for subsequent analyses.

Immunohistochemistry

Whole follicles were fixed in 4% formaldehyde, embedded in paraffin, sectioned at 4 μm, and processed for immunostaining. Deparaffinization and rehydration were achieved through a series of xylene and ethanol washes. Heat-induced antigen retrieval was performed using a Tris-Based Antigen Unmasking Solution (Vector Laboratories; Newark, CA). Endogenous peroxidase activity was quenched by incubating the sections with 1X Quenching Buffer. Sections were then incubated in 2.5% Normal Horse Serum and subsequently with the primary antibody for SOX9. The primary antibody was detected using an ImmPRESS-AP Horse Anti-Rabbit IgG Polymer Detection Kit (Vector Laboratories) and developed with ImmPACT Vector Red (Vector Laboratories) according to the manufacturer's instructions. Slides were counterstained with hematoxylin. Negative control slides were prepared in an identical manner and processed without the primary antibody.

Gene expression analysis

Total RNA was isolated from cumulus cells and hGLCs using the RNeasy mini kit (Qiagen) according to the manufacturer's instructions. First-strand cDNA was synthesized by reverse transcribing 100 ng of total RNA using SuperScript IV with Oligo $(dT)_{20}$ primer and Random Hexamer (Integrated DNA Technologies; Coralville, IA, USA). The mRNA levels of the examined genes were measured by quantitative PCR (qPCR) using Brilliant III Ultra-Fast SYBR Green (Agilent Technologies; Santa Clara, CA, USA) or TaqMan Fast Advanced Master Mix (Applied Biosystems; Waltham, MA, USA). Oligonucleotide primers for each gene were designed using Primer3 software (RRID: SCR_003139) or the Primer-BLAST program (RRID: SCR_003095). For *SOX9* analysis, TaqMan primer (Hs00165814_m1) was used (primer sequence information is provided in the key resources table). The relative abundance of the target transcripts was normalized to *GAPDH* mRNA (Hs00266705_g1) for *in vivo* samples and *GNPDA2* for *in vitro* samples and was calculated according to the Pfaffl method.[63]

Western Blot analysis

Whole-cell extracts were collected from hGLCs utilizing sonication. The extracts were denatured by heating at 95°C for 5 min prior to electrophoresis. The samples were run on a 7.5-10% polyacrylamide gel and subsequently transferred to nitrocellulose membranes. Membranes were blocked with 5% skim milk or BSA in Tris-buffered saline containing 0.1% Tween-20 for 1 h. After blocking, the membranes were incubated overnight at 4°C with the primary antibody against SOX9, STAR, CYP11A1, HSD3B, or ACTB (antibody information is provided in the key resources table). The blots were then incubated with the secondary horseradish peroxidase-conjugated antibody for 1 h at room temperature. Protein bands were detected using the Amersham ECL Prime Western Blotting Detection Reagent, and the signals were visualized using ChemiDoc (Bio-Rad Laboratories, Hercules, CA, USA).

Progesterone assay

The concentration of progesterone was measured using an Immulite kit (Siemens Healthineers; Erlangen, Germany). The assay sensitivity for progesterone was 0.02 ng/mL, with intra- and inter-assay coefficients of variation of 7% and 12%, respectively.

QUANTIFICATION AND STATISTICAL ANALYSIS

Data are presented as mean ± standard error of the mean (SEM). For all data analysis, homogeneity of variance was tested using Levene's test, and log transformations were performed, as appropriate. For *in vivo* data, One-way Analysis of variance (ANOVA) was used to test differences in mRNA levels for each gene across the time of tissue collection. If ANOVA revealed significant effects, Duncan's test was used for mean comparisons, with $p < 0.05$ considered significant. A paired *t*-test was used to test differences in mRNA levels of *SOX9* between cumulus cells and granulosa cells, as well as between the control and hCG stimulation. For experiments involving siRNA treatments, one-way repeated measures ANOVA, followed by paired two-tailed *t*-tests, was used to test differences in progesterone levels or mRNA levels for each gene between treatments within time points. The means were compared, with $p < 0.05$ considered significant. Statistical analysis was performed using IBM SPSS software (vers. 27).